

This discussion paper is/has been under review for the journal Biogeosciences (BG).  
Please refer to the corresponding final paper in BG if available.

# Modeling coral calcification accounting for the impacts of coral bleaching and ocean acidification

C. Evenhuis<sup>1,2</sup>, A. Lenton<sup>1</sup>, N. E. Cantin<sup>3</sup>, and J. M. Lough<sup>3</sup>

<sup>1</sup>Centre for Australian Weather and Climate research, CSIRO, Marine and Atmospheric Research, Hobart, Tasmania, Australia

<sup>2</sup>Now at the Plant Functional Biology and Climate Change Cluster, Faculty of Science, University of Technology, Sydney, NSW, Australia

<sup>3</sup>Australian Institute of Marine Science, PMB 3 Townsville MC, Townsville, QLD 4810, Australia

Received: 13 December 2013 – Accepted: 13 December 2013 – Published: 6 January 2014

Correspondence to: A. Lenton (andrew.lenton@csiro.au)

Published by Copernicus Publications on behalf of the European Geosciences Union.

Title Page

Abstract

Introduction

Conclusions

References

Tables

Figures

◀

▶

◀

▶

Back

Close

Full Screen / Esc

Printer-friendly Version

Interactive Discussion



## Abstract

Coral reefs are diverse ecosystems threatened by rising CO<sub>2</sub> levels that are driving the observed increases in sea surface temperature and ocean acidification. Here we present a new unified model that links changes in temperature and carbonate chemistry to coral health. Changes in coral health and population are able to explicitly modelled by linking the rates of growth, recovery and calcification to the rates of bleaching and temperature stress induced mortality. The model is underpinned by four key principles: the Arrhenius equation, thermal specialisation, resource allocation trade-offs, and adaption to local environments. These general relationships allow this model to be constructed from a range of experimental and observational data. The different characteristics of this model are also assessed against independent data to show that the model captures the observed response of corals. We also provide new insights into the factors that determine calcification rates and provide a framework based on well-known biological principles for understanding the observed global distribution of calcification rates. Our results suggest that, despite the implicit complexity of the coral reef environment, a simple model based on temperature, carbonate chemistry and different species can reproduce much of the observed response of corals to changes in temperature and ocean acidification.

## 1 Introduction

Coral reefs are among the most biologically complex ecosystems, supporting a diverse range of species, and providing critically important ecosystem services such as food, resources for livelihoods and coastal protection. Despite this, they are facing an unprecedented rate of environmental change in response to increasing atmospheric CO<sub>2</sub> levels driving observed increasing ocean temperatures and ocean acidification (Hoegh-Guldberg et al., 2011; Doney et al., 2009).

**BGD**

11, 187–249, 2014

## Modeling coral calcification

C. Evenhuis et al.

Title Page

Abstract

Introduction

Conclusions

References

Tables

Figures

⏪

⏩

◀

▶

Back

Close

Full Screen / Esc

Printer-friendly Version

Interactive Discussion



**Modeling coral calcification**

C. Evenhuis et al.

[Title Page](#)[Abstract](#)[Introduction](#)[Conclusions](#)[References](#)[Tables](#)[Figures](#)[◀](#)[▶](#)[◀](#)[▶](#)[Back](#)[Close](#)[Full Screen / Esc](#)[Printer-friendly Version](#)[Interactive Discussion](#)

The ocean plays a key role in slowing the rate of climate change by absorbing and sequestering approximately 25–30% of the annual atmospheric carbon dioxide (CO<sub>2</sub>) emissions (Le Quéré et al., 2013). As CO<sub>2</sub> enters the ocean (slowing the rate of ocean warming) a number of changes in seawater chemistry occur, collectively referred to as ocean acidification (OA). For Scleractinian corals one of the most significant consequences of OA is the decrease in the concentration of carbonate ions (CO<sub>3</sub><sup>2-</sup>), which together with calcium are used to construct their skeletons. The primary mineral phase of calcium carbonate formed by Scleractinian corals is aragonite. Studies have demonstrated that the capacity of corals to calcify is reduced as the saturation state of aragonite ( $\Omega_{\text{arg}}$ ) declines in response to rising CO<sub>2</sub> concentrations in seawater (Schneider and Erez, 2006; Langdon and Atkinson, 2005; Pandolfi et al., 2011). Projections suggest that future rates of coral reef community dissolution may exceed rates of CaCO<sub>3</sub> production (calcification), leading to net loss of reef framework and coral reef habitat within this century (Silverman et al., 2009; Hoegh-Guldberg et al., 2007).

As atmospheric CO<sub>2</sub> and other greenhouse gas concentrations continue to rise, ocean temperatures will continue to increase e.g. in the tropical ocean, where the greatest abundance and diversity of corals are found, a net increase of 0.09°C/decade in the period 1950–2011 has been reported (Lough, 2012). Scleractinian corals are sensitive to increasing ocean temperatures because of the close symbiotic relationship between the coral host and their endosymbiotic dinoflagellate (*Symbiodinium* spp.). Experimental studies have shown that calcification is enhanced as temperature increases, up to an optimum value that is typically a few degrees below the seasonal maximum temperature, and beyond this optimum temperature calcification rates rapidly decline (Al-Horani, 2005; Cooper et al., 2008; Cantin et al., 2010). This increase in temperature will ultimately lead to corals ejecting their symbiont dinoflagellates, zooxanthellae, in a process known as bleaching. Without the photosynthetic products produced by the symbiont many essential physiological processes such as calcification and reproduction, are suppressed (Rodrigues and Grotzoli, 2006; Carilli et al., 2009; Cantin et al., 2010). Observations suggest there has been an increase in the frequency and inten-

sity of global mass bleaching events in recent decades resulting in an estimated loss in hard coral cover of approximately 18 % and a decline in the dominant populations at a rate of 1–2 % per year (Hoegh-Guldberg et al., 2011; Wilkinson, 2008).

Historically, the risk of corals bleaching due to extreme temperatures has been modeled by the degree heating week or month metrics e.g. Donner et al. (2005). Because these metrics were built on empirical observations of bleaching they can be viewed as a statistical heuristic. It is therefore difficult to link degrees heating metrics to the changes in biological function that result from stress, or to extend the metrics to include differential species response or to account for thermal adaptation. As a consequence, it is difficult relate how the risk of bleaching given by the DHW metric impacts calcification rates e.g. Buddemeier et al. (2008). Furthermore, there are a number of ways for estimate the thermal thresholds that underpin the DHW metric, and little consensus exists as to which approach is best suited to a given location. Studies have shown that the projected responses of coral reefs in some regions are highly sensitive to way the thermal threshold is calculated (Donner, 2011), and the distribution and severity of coral bleaching throughout individual coral reefs can be extremely patchy (Baird and Marshall, 2002; Berkelmans et al., 2004). Studies investigating the past and future response of corals usually focus on the impact of increasing ocean temperatures leading to bleaching (Cantin et al., 2010; van Hooidonk et al., 2013; Frieler et al., 2013) or on ocean acidification (Ricke et al., 2013).

In this work we acknowledge that coral reefs are very complex ecosystems and any complete model would require describing a vast array of processes ranging from global scale climate systems down to wave action on the local reef scale, and capturing the closely coupled interaction between hundreds of species of plants and animals. At present such a model at the reef scale is both beyond our current theoretical understanding (Gustafsson et al., 2013). However, as the reef ecosystem is contingent on the calcium carbonate production from reef-building corals, as a first approximation, the construction of the reef can be treated separately from the rest of the ecosystem.

## BGD

11, 187–249, 2014

### Modeling coral calcification

C. Evenhuis et al.

Title Page

Abstract

Introduction

Conclusions

References

Tables

Figures

◀

▶

◀

▶

Back

Close

Full Screen / Esc

Printer-friendly Version

Interactive Discussion



This “bottom up” approach allows the response of coral ecosystems to climate change to be inferred from changes in the rate at which corals calcify.

In this paper we present a new model that provides a unified description of coral calcification linking bleaching-related mortality, recovery from bleaching, and growth.

Our goal is to provide a simple description of these processes that is motivated by the underlying physiological mechanisms and, where possible, validated against experimental observations. The model aims to provide a unified approach to modeling coral growth and health that captures the differences between species and across locations. One of the important features of our model is how the two critical thresholds that define the temperature response are determined by assuming that corals have evolved to maximize their growth over the historical period. By taking into account ocean acidification and temperature our model is able to better resolve the relative influence of these two stressors.

The paper is structured as follows; the methods section describes the formulation of the model and estimation of parameter values based on a synthesis of existing observational and experimental data. In the results section the new model is assessed against independent data that was not used in the formulation of the model. We show that, despite the implicit complexity of the coral reef environment, a simple model based on temperature, carbonate chemistry and different species can reproduce much of the observed coral response. We also demonstrate how the model provides insights into processes that give rise to the linear relationship between average temperature and calcification rate observed by Lough and Barnes (2008) and Lough (2008). Finally in the discussion we compare this new model to existing models that combine ocean acidification and temperature, discuss the limitations of our model, and identify key areas for future research.

**BGD**

11, 187–249, 2014

## Modeling coral calcification

C. Evenhuis et al.

Title Page

Abstract

Introduction

Conclusions

References

Tables

Figures

⏪

⏩

◀

▶

Back

Close

Full Screen / Esc

Printer-friendly Version

Interactive Discussion



## 2 Methods – model construction

In this section we describe how our new model of calcification rate is constructed (Eq. 1). This model aims to capture the general, transferable relationships between growth, bleaching and calcification based on experiments and observations of corals from different locations and from different taxa. The calcification rate ( $G$ ) is given in Eq. (1).

$$\dot{G} = g_C \frac{\text{Irradiance}}{\bar{Q}^{\text{day}}} \underbrace{\alpha(T, T_{\text{opt}}, \Delta T)}_{\text{Adapted response}} \underbrace{\beta(T_{\text{opt}}, E_a)}_{\text{Thermal envelope}} \underbrace{\gamma(\Omega; \Omega_{\text{cp}}, \kappa)}_{\text{Aragonite dependence}} C_{\text{sp}} P_H \quad (1)$$

Calcification rate
Calcification constant
Temperature dependence
Aragonite dependence
Species constant
Population of healthy coral

The calcification rate depends on the level of light ( $\bar{Q}^{\text{day}}$ ), the sea surface temperature ( $\alpha, \beta$ ), the aragonite saturation state ( $\gamma$ ), whether the species is fast or slow growing ( $C_{\text{sp}}$ ), and on the population of healthy corals ( $P_H$ ). The effect of light is accounted for by using the expression for the daily average solar irradiation that depends only the day of the year and latitude.

One of the novel aspects of this model is the inclusions of the way in which corals respond to temperature. The commonalities in the temperature response between species have been extensively investigated using the *Metabolic Theory of Ecology* (Dell et al., 2011; Brown et al., 2004) and *Dynamic Energy Budget* (Nisbet et al., 2000) frameworks. In the case of corals, the temperature dependence is more complicated as normal physiological performance relies on the symbiotic relationship between the coral polyp and the algal dinoflagellate, *Symbiodinium*. This complication is reflected in the sophistication of coral models that model host and symbiont responses (Muller et al., 2009; Gustafsson et al., 2013). Here we quantify how the holobiont (i.e. the coral and symbiont treated as a single entity) responds to temperature and aragonite saturation state. The temperature response is modelled as the product of two terms, the adapted response  $\alpha$ , and thermal envelope  $\beta$ . A key part of the model is how growth,

bleaching, recovery and calcification depend on temperature and differ systematically between species.

We will now explain each of the terms in Eq. (1), first quantifying the response of corals to aragonite saturation state  $\gamma$ , after which the form of the adapted temperature response  $\alpha$  is established. This allows the equations that describe changes in the population and health of individual corals (including  $P_H$  and  $C_{sp}$ ) to be determined. Subsequently, by linking the population changes to the local temperature regime a general method for finding the adapted range ( $T_{opt}, \Delta T$ ) is developed. Finally, by relating the rates of calcification between different reefs, the form of the thermal envelope is set ( $\beta$ ).

## 2.1 Aragonite dependence ( $\gamma$ )

Coral reefs are primarily composed of aragonite, the metastable form of calcium carbonate produced by hermatypic corals. Calcification rates are commonly related to the aragonite saturation state ( $\Omega_{arg}$ ), which is a measure of the inorganic solution equilibrium between solid aragonite and calcium and carbonate ions in solution. The dependence of the calcification rate with the seawater carbon system has been extensively investigated (Erez et al., 2011; Pandolfi et al., 2011; Schneider and Erez, 2006; Putron et al., 2010) but remains poorly understood. Experiments have shown that corals transport seawater to the site of calcification within the basal calcicoblastic ectoderm and are able to manipulate its carbonate chemistry, thereby up-regulating the aragonite saturation state in favour of  $\text{CaCO}_3$  precipitation (Al-Horani, 2005). The precipitation of aragonite at the site of calcification may be inorganic, biologically mediated or some combination thereof (Allemand et al., 2011). Given these complexities, our model employs an empirical relationship to describe how calcification depends on the aragonite saturation state of seawater.

To determine the functional form of  $\gamma$  (Eq. 1) we examined experiments in which calcification rates are measured while holding the temperature constant. The upper panel of Fig. 1 shows the relationship between calcification rate and aragonite saturation

**BGD**

11, 187–249, 2014

## Modeling coral calcification

C. Evenhuis et al.

Title Page

Abstract

Introduction

Conclusions

References

Tables

Figures

◀

▶

◀

▶

Back

Close

Full Screen / Esc

Printer-friendly Version

Interactive Discussion



tion state for 18 experiments, from which two broad classes of response are evident (an example of a more comprehensive list of experiments can be found in Table 2 of (Erez et al., 2011)). In the first class (drawn in blue), calcification declines linearly with aragonite saturation, ceasing around  $\Omega \approx 1$ . While in the second class (drawn in red), the response is more plateaued. The response is comparably more flat around  $\Omega = 3.5$  and a steep fall off when  $\Omega < 1$ . The reason for the two responses is not yet understood (for a recent review see Chan and Connolly, 2013). Current hypotheses include differences in experimental techniques, differences between tropical and temperature corals, and whether the corals were given sufficient time to adapt to the change in sea-water chemistry. However, the available experimental evidence suggests that the linear response is most likely related to nutrient concentrations (Pandolfi et al., 2011).

The observed linear and plateaued responses are fitted to a modified version of the Michaelis–Menten curve. This curve is widely used to describe biochemical reactions that are enzyme mediated. Initially this curve increases linearly, after which it saturates and approaches an asymptotic value. The following function (Eq. 2) is used to fit the dependence of calcification on Aragonite saturation state:

$$\underbrace{\gamma(\Omega; \Omega_c, \kappa)}_{\text{Aragonite dependence}} = \underbrace{\frac{\Omega - 1 + 0.1\kappa}{1 + \kappa(\Omega - 1 + 0.1\kappa)}}_{\text{Modified Michaelis–Menten}} \underbrace{\frac{1 + \kappa(\Omega_c - 1 + 0.1\kappa)}{\Omega_c - 1 + 0.1\kappa}}_{\text{Cross-over point}} \underbrace{\frac{1}{3.5 - 1}}_{\text{Normalisation}} \quad (2)$$

This functional form is controlled by two parameters;  $\kappa$  determines the curvature, and  $\Omega_c$  sets the point at which curves with different values of  $\kappa$  intersect. The upper panel of Fig. 1 plots the 18 experimental calcification rates, normalised so that at  $\Omega = 3.5$  the calcification rate is 100%. This normalisation means that the cross-over point for both responses is also  $\Omega_c = 3.5$ . If  $\kappa = 0$  2.1 simplifies to  $(\Omega - 1) \frac{1}{3.5 - 1}$ , which is the linear response that starts at  $\Omega = 1$  and is normalised to 100% at  $\Omega = 3.5$ . In Fig. 1 it can be seen how increasing  $\kappa$  increases the curvature of the response, and how the  $0.1\kappa$  term shifts the point at which the curve goes to zero. This effect is most apparent for  $\kappa = 5$

## BGD

11, 187–249, 2014

### Modeling coral calcification

C. Evenhuis et al.

Title Page

Abstract

Introduction

Conclusions

References

Tables

Figures

◀

▶

◀

▶

Back

Close

Full Screen / Esc

Printer-friendly Version

Interactive Discussion



for which calcification ceases at  $\Omega = 0.5$ . By fitting the  $\gamma$  to the plateaued experimental results we determined that a typical value for the curvature is  $\kappa = 2$ .

In the lower panel of Fig. 1 the results of Langdon and Atkinson (2005) and Holcomb et al. (2012) are used to determine the cross-over point. These experiments measured calcification rates under both nutrient poor and replete conditions. A linear response was observed in nutrient poor conditions, whilst a plateaued response was observed in replete conditions. The results are normalised so that the (linear) responses is 100% when  $\Omega = 3.5$ . By fitting the curve for  $\gamma$  with  $\kappa = 2$  to the nutrient replete results the crossover point was determined to be  $\Omega_{cp} = 2.6$ .

In the upper panel of Fig. 1 there is a considerable spread in the results. Most of these experiments measure net calcification rate, which includes negative effects from processes such as dissolution. Although it is difficult to estimate the magnitude of the dissolution rate, it is expected to be larger for in situ measurements than for laboratory experiments, given the processes that control dissolution e.g. Andersson and Gledhill (2013).

By comparing with experimental measurements of calcification rates it was possible to reduce the aragonite response  $\gamma$  to one of two possibilities, a linear ( $\kappa = 0$ ) and plateaued ( $\kappa = 2$  and  $\Omega_{cp} = 2.6$ ) response (Fig. 1). Unless indicated otherwise, the linear calcification response is used, however a plateaued response could be substituted as desired.

## 2.2 Modelling the temperature and population responses ( $\alpha, \beta, C_{sp}, P_H$ )

The temperature response (in Eq. 1) is comprised of both the adapted response ( $\alpha$ ) and thermal envelope ( $\beta$ ). The adapted response captures how corals respond to temperature fluctuations on timescales of hours to weeks, and dictates the temperature range over which symbiosis occurs. The adapted response can be considered as the fast response, while the thermal envelope refers to the longer-term response. Specifically, the thermal envelope describes how an increase in the rate of biochemical reactions increases as the temperature rises and more thermal energy becomes available.

BGD

11, 187–249, 2014

## Modeling coral calcification

C. Evenhuis et al.

Title Page

Abstract

Introduction

Conclusions

References

Tables

Figures

◀

▶

◀

▶

Back

Close

Full Screen / Esc

Printer-friendly Version

Interactive Discussion



Broadly speaking, experimental observations of coral can be viewed as probing either the adapted response or the thermal envelope. Laboratory experiments that manipulate temperature and measure the change in coral's biological functions explore the adapted response. While studies that compare the historical rates of coral calcification from locations with different climates can be used to infer the thermal response. Separating these responses by their time scales allows us to quantify key information about the response of individual coral species ( $C_{sp}$ ) and the health of the population to changes to temperature ( $P_H$ ).

### 2.2.1 The adapted temperature response ( $\alpha$ )

The adapted response describes how symbiosis in coral is affected by temperature fluctuations on daily to monthly timescales. Although the shape of the adapted response is general, specifics such as the adapted low ( $T_{lo}$ ) and high temperatures ( $T_{hi}$ ) depend on reef location. The shape of the adapted response is based on experimental observations of a range of processes, including photosynthesis (Jones et al., 1998), calcification (Al-Horani, 2005; Jokiel and Coles, 1977), growth (Edmunds, 2005), reproduction (Jokiel and Guinther, 1978) and respiration (Edmunds, 2008). All of these traits exhibit a common behaviour; the rate reaches a maximum at an optimum temperature and steeply decreases to zero on either side to define the adapted temperature range. The similarities in the response across a range of biological processes in corals suggests that these processes most likely respond in unison to the breakdown of symbiosis which we model with the adapted response function,  $\alpha$ .

Mathematically,  $\alpha$  (in Eq. 1) is constructed as a piecewise smooth combination of a cubic polynomial and a constant as shown in Eq. (3):

$$\alpha(T; T_{opt}, \Delta T) = \begin{cases} T > T_{lo} : \overset{\text{Cubic Polynomial}}{-c(T - T_{lo}) \left( (T - T_{lo})^2 - \Delta T^2 \right)} \overset{\text{Normalisation}}{\frac{4}{\Delta T^{4-\delta}}} \\ T < T_{lo} : \underset{\text{Constant}}{-\alpha_{max}} \end{cases} \quad (3)$$

BGD

11, 187–249, 2014

## Modeling coral calcification

C. Evenhuis et al.

Title Page

Abstract

Introduction

Conclusions

References

Tables

Figures

◀

▶

◀

▶

Back

Close

Full Screen / Esc

Printer-friendly Version

Interactive Discussion



where:

$$T_{lo} = T_{opt} - \frac{1}{\sqrt{3}}\Delta T$$

$$T_{hi} = T_{lo} + \Delta T$$

5 The maximum of this function is at  $T_{opt}$ , and is positive between  $T_{hi}$  and  $T_{lo}$ . This function depends on only the adapted range, which can be expressed as  $(T_{lo}, T_{hi})$  or  $(T_{opt}, \Delta T)$ . When the temperature is in this range corals grow, calcify, reproduce and recover from bleaching, whilst outside of this range, bleaching and mortality occur. Consistent with observations the magnitude of the slope at  $T_{hi}$  is twice that at  $T_{lo}$  e.g. Al-Horani (2005).

10 Figure 2 shows the fit of the adapted range ( $\alpha$ ) functional form to the experimental measurements of Al-Horani (2005). The normalisation term (Eq. 3) plays a central role by rewarding thermal specialisation. The rationale behind this term and its effect are discussed fully in Sect. 2.2.7. Although other researchers have modelled temperature response of corals with cubic polynomials, we found that the additional constraints imposed on the form of  $\alpha$  aid in the interpretation and comparison of experimental results.

## 2.2.2 Modelling changes in population ( $P_H$ )

A core part of this model is its ability to describe changes in the health and population of corals. The model uses coral cover as a state variable, which is further classified into four states: healthy, recovering, stressed, and bleached. The four states come from reports of coral condition from the literature (e.g. Reef Base: [www.reefbase.org](http://www.reefbase.org)). The states can be viewed as a qualitative measure of the health of the symbiosis, capturing more quantitative measures such as density of the zooxanthellae or levels of lipid stores.

25 The four states and the transitions between them are shown schematically in Fig. 3 and summarised as follows:

**BGD**

11, 187–249, 2014

**Modeling coral calcification**

C. Evenhuis et al.

- Healthy corals grow and calcify at normal rates. When stressed, healthy corals turn pale.
- Pale corals have ejected some or all of their zooxanthellae, and growth calcification are impaired. When stress is prolonged, pale corals will further bleach, but under normal temperatures pale corals transition to recovering phase of rebuilding tissue reserves.
- Bleached corals have lost the majority of their zooxanthellae, do not grow or reproduce, and face the risk of mortality. Under normal temperatures bleached corals transition to pale, while further stress leads to mortality.
- Recovering corals are those that have only recently reacquired zooxanthellae after bleaching, and although healthy in appearance, do not reproduce or calcify at the same level as healthy corals. When stressed, recovering corals turn pale, otherwise they return to healthy under normal conditions.

The transition between the states is modelled by a system of 1st order differential equations. The rate of these transitions is modulated by a common temperature response, and by the general patterns of bleaching susceptibility that have been observed between coral species. The set of equations described in this section for bleaching and recovery are determined from the work of Jokiel and Coles (1977) who investigated the calcification, bleaching and recovery rates of three Hawaiian coral species.

[Title Page](#)[Abstract](#)[Introduction](#)[Conclusions](#)[References](#)[Tables](#)[Figures](#)[⏪](#)[⏩](#)[◀](#)[▶](#)[Back](#)[Close](#)[Full Screen / Esc](#)[Printer-friendly Version](#)[Interactive Discussion](#)

### 2.2.3 Bleaching

The transition of coral from healthy ( $\dot{P}_H$ ) to pale ( $\dot{P}_P$ ), to bleached ( $\dot{P}_B$ ), and finally to dead is given by the following first order differential equation:

$$\begin{pmatrix} \dot{P}_H \\ \dot{P}_R \\ \dot{P}_P \\ \dot{P}_B \end{pmatrix} = \underbrace{g_B}_{\text{Bleaching constant}} \underbrace{C_{sp}}_{\text{Species constant}} \underbrace{\frac{\text{Insolation}}{\bar{Q}_{\text{day}}}}_{\text{Insolation}} \underbrace{\left[ \begin{array}{c} \text{Temperature dependence} \\ \alpha(T, T_{\text{opt}}, \Delta T) \quad \beta(T_{\text{opt}}, E_a) \\ \text{Adapted response} \quad \text{Thermal envelope} \end{array} \right]}_{\text{Temperature dependence}} \begin{pmatrix} +1 & 0 & -1 & 0 \\ 0 & 0 & 0 & 0 \\ 0 & 0 & \frac{1}{2} & -\frac{1}{2} \\ 0 & 0 & 0 & +\frac{1}{4} \end{pmatrix} \begin{pmatrix} P_H \\ P_R \\ P_P \\ P_B \end{pmatrix} \quad (4)$$

Where the constant  $g_B$  determines the time scale of the bleaching which is applicable for all locations and species,  $C_{sp}$  is the species constant, and  $\alpha$  and  $\beta$  are the transient and steady state temperature response curves, respectively. Importantly, the rate of bleaching is proportional to the species constant ( $C_{sp}$ ). For example, faster growing corals will bleach faster and have higher mortality, while slower growing corals will be more resistant to bleaching, consistent with observations. This differential response to temperature or ( $C_{sp}$ ) can be understood in an energy budget framework as a trade-off between growth and heat tolerance. There is a wide range of mechanisms and strategies that corals can use to mitigate the damage from bleaching. For example, corals that store more lipids or have more tissue biomass are able to better survive bleaching (Anthony et al., 2009), the coral and the symbiont may employ anti-oxidants to deal with the increase in reactive oxygen production or express heat shock proteins to deal with the increased temperature (Baird et al., 2009), or corals may increase feeding rates to meet the short fall in autotrophic energy (Houlbreque and Ferrier-Pages, 2009). However, any strategies that a coral employs to defend against heat stress, energy deficiencies impact on the energy budget and reduce the allocation of resources to growth and reproduction (Rodrigues and Grottoli, 2006; Michalek-Wagner and Willis, 2001).

The transitions between the four coral states, shown schematically in Fig. 3, correspond to the entries in the  $4 \times 4$  matrix in Eq. (4). The first row of Fig. 4 shows the fit

BGD

11, 187–249, 2014

Modeling coral calcification

C. Evenhuis et al.

Title Page

Abstract

Introduction

Conclusions

References

Tables

Figures

◀

▶

◀

▶

Back

Close

Full Screen / Esc

Printer-friendly Version

Interactive Discussion



of the adapted response curve to the measurements of calcium carbonate calcification rate from Jokiel and Coles (1977). This allowed the adapted temperature range ( $T_{lo}, T_{hi}$ ) and the species constant ( $C_{sp}$ ) to be determined for each coral species. As thermal response in these short-term experiments plays no role we ignore this response and set the thermal envelope to  $\beta \approx 1$ . The species parameter was defined to be 1.0 for *P. damicornis* corals. As adapted range is the same for the three corals,  $T_{opt}$  the rates of the transition (healthy to pale, pale to bleached, bleached to dead) can be determined by fitting the model to the experimental observations for *P. damicornis*. The agreement between the resulting patterns from the model output and the experimental observations is very good (Fig. 4), and the bleaching constant is calculated to be  $g_B = 8.d^{-1}$ . This allowed the species constants for *M. verrucosa* ( $C_{sp} = 2$ ) and *F. scutaria* ( $C_{sp} = 0.9$ ) to be calculated.

## 2.2.4 Recovery from bleaching

After exposure to elevated temperatures, corals undergo a range of recovery processes (Fig. 3). Following bleaching the coral host acquires significantly less autotrophic carbon based energy from the depleted symbiont community within in its tissue (see review by Glynn, 1996). As recovery processes continue following thermal stress, the coral host metabolizes tissue reserves and relies on heterotrophic feeding to compensate for energy limitations (Thornhill et al., 2011). Rate of recovery processes which include, repopulation of the symbiont community, tissue repair and replenishing energetic tissue reserves will depend upon the severity of the thermal stress and the colony condition prior to the thermal stress event. Collectively these recovery processes are modelled using the following set of 1st order differential equations (Eq. 5), which differ from Eq. (3) with the addition of an additional recovering state ( $\dot{P}_R$ ). This describes corals which are in the recovering state and, despite having a healthy appearance, display suppressed calcification, growth and reproduction (Rodrigues and Grottoli, 2006). Figure 3 shows the comparison between the model output using Eqs. (4.1) and (4.2). Noting that the modelling results show the recovering state ( $\dot{P}_R$ ), which was not re-

BGD

11, 187–249, 2014

## Modeling coral calcification

C. Evenhuis et al.

Title Page

Abstract

Introduction

Conclusions

References

Tables

Figures

◀

▶

◀

▶

Back

Close

Full Screen / Esc

Printer-friendly Version

Interactive Discussion



ported in the experimental results of Jokiel and Coles (1977).

$$\begin{pmatrix} \dot{P}_H \\ \dot{P}_R \\ \dot{P}_P \\ \dot{P}_B \end{pmatrix} = g_M \underset{\substack{\text{Mortality} \\ \text{constant}}}{C_{sp}} \frac{\text{Insolation}}{Q} \begin{pmatrix} 0 & 0 & 0 & 0 \\ 0 & 0 & 0 & 0 \\ 0 & 0 & 0 & 0 \\ 0 & 0 & 0 & -1 \end{pmatrix} \begin{pmatrix} P_H \\ P_R \\ P_P \\ P_B \end{pmatrix} \quad (5)$$

$$+ g_R \underset{\substack{\text{Recovery} \\ \text{constant}}}{C_{sp}} \frac{\text{Insolation}}{Q} \overbrace{\begin{pmatrix} \alpha(T, T_{opt}, \Delta T) & \beta(T_{opt}, E_a) \\ \text{Adapted response} & \text{Thermal envelope} \end{pmatrix}}^{\text{Temperature dependence}} \begin{pmatrix} 0 & +\frac{1}{2}C_{sp} & 0 & 0 \\ 0 & -\frac{1}{2}C_{sp} & +C_{sp} & 0 \\ 0 & 0 & -C_{sp} & +8/C_{sp} \\ 0 & 0 & 0 & -8/C_{sp} \end{pmatrix} \begin{pmatrix} P_H \\ P_R \\ P_P \\ P_B \end{pmatrix}$$

5 Again, the form of the equations was determined by fitting to the results of Jokiel and Coles (1977), the values of the continued mortality and recovery time constants were determined as  $g_M = 0.04d^{-1}$  and  $g_R = 0.2d^{-1}$ . The first term in Eq. (5) represents the continued risk of mortality that bleached corals face even when the temperature falls back into the adapted range, and reflects the limited ability of corals to survive without zooxanthellae. This term is also proportional to the species constant  $C_{sp}$ , as  
 10 slower growing corals have larger lipid stores that enable them to survive longer without zooxanthellae. The second term in Eq. (5) represents the recovery from bleaching as the corals return from bleached to pale, pale to recovering, and finally to healthy. The bleached to pale transition term differs from the other terms, as it is inversely proportional to the species constant. This means that, in general, faster growing corals react  
 15 more negatively to bleaching (more rapid bleaching, increased risk of mortality when bleached and slower to re-establish symbiosis), the exception being that the transition from pale to healthy is more rapid in faster than in slower growing corals. At present, without additional data on recovery dynamics it is difficult to determine whether this is an artefact resulting from over fitting the uncertainties in the experimental data or whether this reflects an intrinsic difference between the biological processes that take place during recovery.  
 20

Figure 3 shows the comparison between the model output using Eqs. (4.1) and (4.2). Noting that the modelling results show the recovering state ( $\dot{P}_R$ ), which was not reported in the experimental results of Jokiel and Coles (1977).

### 2.2.5 Growth constant ( $G_C$ )

5 The coral growth term in the model has the highest uncertainty as it represents the combined effect of many processes. This term (Eq. 6) encompasses the growth of individual corals, natural mortality, recolonisation of dead coral structures, reproduction and constraints on growth from the maximum habitat size are all described by a single equation for growth in our model. The equation used for the growth term in the model  
10 is given in Eq. (6).

$$\begin{pmatrix} \dot{P}_H \\ \dot{P}_R \\ \dot{P}_P \\ \dot{P}_B \end{pmatrix} = g_C \underbrace{C_{sp}}_{\text{Bleaching constant}} \underbrace{Q}_{\text{Species constant}} \underbrace{\frac{\text{Insolation}}{\text{day}}}_{\text{Temperature dependence}} \underbrace{\alpha(T, T_{opt}, \Delta T)}_{\text{Adapted response}} \underbrace{\beta(T_{opt}, E_a)}_{\text{Thermal envelope}} \quad (6)$$

$$\cdot \underbrace{\left( K - \sum P_i \right)}_{\text{Logistic bottleneck}} \begin{pmatrix} +1 & 0 & 0 & 0 \\ 0 & 0 & 0 & 0 \\ 0 & 0 & 0 & 0 \\ 0 & 0 & 0 & 0 \end{pmatrix} \begin{pmatrix} P_H \\ P_R \\ P_P \\ P_B \end{pmatrix}$$

15 The term  $(K - \sum P_i)$  is referred to as the *logistic growth* in ecological modelling serves to reduce the growth rate as the total population ( $\sum P_i$ ) as it approaches the carrying capacity ( $K$ ) of the location. In this work  $K = 1$  (i.e. 100 % carrying capacity), however there is scope to model external stressors that could reduce the carrying capacity of a location, such as storm damage or sea-level rise, by allowing  $K$  to vary temporally.

20 The range of values for the growth constants is large (Table 2) as there are many contributing factors to this term such as whether the measurements are taken in laboratory conditions that remove stressors that in situ coral observations record. While it is

very hard to get a firm estimate of this parameter, we selected the value of the growth constant ( $g_C$ ) to be  $0.002d^{-1}$ , based on a synthesis of in situ published that report the return of coral coverage after a disturbance such as bleaching.

### 2.2.6 Species response ( $C_{sp}$ )

5 Studies have identified the role of species as a confounding variable when comparing observations of corals. In the previous section differences between species were captured in the model by the species constant  $C_{sp}$  that modulates the relative rates of key processes. As discussed previously, corals that grow and calcify faster and are more sensitive to bleaching are modelled as having  $C_{sp} > 1$ , whilst corals that calcify and grow slower but are more resistant to bleaching are modelled as having  $C_{sp} < 1$ .  
10 Therefore it is useful to an estimate of the expected range of the species constant. In the previous sections the species constant was determined from direct measurements of the calcification rate, which in turn was used to infer the relative rates of growth, bleaching and recovery.

15 In this section an estimate of the species constants of a wide range of coral species is derived from observations of the large-scale bleaching that occurred in 1998 on GBR (Marshall and Baird, 2000). These allow the species of coral to be linked to the species constant  $C_{sp}$  and can serve as a guide when setting up the model for a specific coral reef. Figure 6 compares the bleaching observations to the model output for a range  
20 of the species constants. The adapted temperature range of  $T_{lo} = 20.0$  and  $T_{hi} = 30.6$  used in the model was estimated from historical temperatures from the Hadley SST (Rayner et al., 2003) product and from reported bleaching events from ReefBase (www.reefbase.org). The model was run from 1 January 1998 to 12 March 1998 using in situ recorded temperature for Pelorus Reef (available from the Australian Institute of  
25 Marine Science website). It can be seen that the value of the species constant varied from 0.2 to 4 (Fig. 6) and covers the observed range in bleaching response. Although the agreement between observations and model output for the percentages of healthy and dead corals is generally good, the pale and bleached categories systemically differ.

## Modeling coral calcification

C. Evenhuis et al.

Title Page

Abstract

Introduction

Conclusions

References

Tables

Figures

◀

▶

◀

▶

Back

Close

Full Screen / Esc

Printer-friendly Version

Interactive Discussion



This maybe explained by differences in how pale and bleached corals were classified in this study from the classification of Jokiel and Coles (1977) that was used to construct this model.

The differences in bleaching response between species may also, in part, be due to differences in the depths at which the species lived, as shown for *Montastrea annularis* (Baker and Weber, 1975). By way of illustration, consider two corals that have an identical bleaching response ( $T_{lo}$ ,  $T_{hi}$ , and  $C_{sp}$ ); one is found in shallow water whilst the other is found only in deeper water. The shallower coral will be exposed to a larger range of temperatures and higher light intensities, therefore, will bleach to a greater degree than the deeper coral. Field based observations also indicate that bleaching is generally most severe on reef flat and upper reef slope habitats, to a depth of  $\sim 4-6$  m (Oliver and Berkelmans, 1999). As we do not explicitly include depth in the model it appears that the deeper corals will be more tolerant to bleaching, i.e. that  $C_{sp}$  is lower for coral species that are typically found in deeper habitats.

### 2.2.7 Determining the adapted temperature range ( $\alpha$ )

It has been widely observed that coral bleaching thresholds are only a few degrees above and below the extremes of the local temperatures, which implies that corals are facing a high risk of bleaching as temperatures change (Hoegh-Guldberg, 1999). From this observation two conclusions are drawn that are central to the model. Firstly, corals are able to adapt to their local environment by changing their adapted response ( $\alpha$ ). And secondly, corals must derive some benefit from having their thermal threshold close to temperature extremes that offsets the increased risk of bleaching. This motivates the inclusion of a reward for thermal specialisation within the model.

$$\alpha(T; T_{opt}, \Delta T) = \begin{cases} T > T_{lo} : -c(T - T_{lo}) \left( (T - T_{lo})^2 - \Delta T^2 \right) \frac{4}{\Delta T^{4-\delta}} & \text{Cubic Polynomial Normalisation} \\ T < T_{lo} : -\alpha_{\max} & \text{Constant} \end{cases} \quad (7)$$

5

10

15

20

25

where:

$$T_{lo} = T_{opt} - \frac{1}{\sqrt{3}}\Delta T$$

$$T_{hi} = T_{lo} + \Delta T$$

5 Based on the wide diversity within the Symbiodinium genus (Baker, 2003; Jones, 2008), corals have the potential to specialise through symbiosis. This can be considered as a resource allocation issue; i.e. the changes a coral undergoes to adapt to a wide temperature range, be it biochemical or physiological, will come at some cost to the coral. The normalisation term in Eq. (7) describes this thermal specialisation, through either  
10 rewarding or penalising coral calcification rates. In the model large adapted temperature range results in reduced rates of growth and calcification, which is consistent with the hypothesis of (Oliver and Palumbi, 2011) and (Castillo et al., 2012).

The simplest way to reward thermal specialisation is to conserve the area under the adapted response curve (i.e. to normalise the function  $\alpha$  over the temperature  $T_{lo}$  to  $T_{hi}$ ). If the area under  $\alpha$  is conserved then the maximum of  $\alpha$  is proportional to  $\Delta T^{-1}$ . If identical corals from two sites are compared and the second site has twice the temperature range of the first, the model would predict that the rates of growth and calcification at the second site would be half that of the first site. This is a common choice for normalisation of reaction norms, for example see Gilchrist (1995). The effect  
20 of thermal specialisation is illustrated in Fig. 7 which shows how calcification rates are reduced as the adapted range increases.

Having established how thermal specialisation is rewarded, the procedure for finding the adapted range of corals is now outlined ( $T_{lo}$ ,  $T_{hi}$ ). By assuming that the corals have adapted to their local climate the adapted temperature range can be found by maximising the calcification rate over an historical period. Strictly speaking calcification is not  
25 a measure of Darwinian fitness. However, the simplicity of the model means that reproduction is not modelled explicitly (reproduction is implicitly modelled by the logistical

Modeling coral calcification

C. Evenhuis et al.

Title Page

Abstract

Introduction

Conclusions

References

Tables

Figures

◀

▶

◀

▶

Back

Close

Full Screen / Esc

Printer-friendly Version

Interactive Discussion



equation), which leaves calcification as the best available variable to serve as a proxy for Darwinian fitness.

Maximising the total calcification rate finds the best trade-off between the competing effects of bleaching (which favours a large adapted range) and thermal specialisation (which favours a small adapted range). Figure 7 gives an illustration of this trade-off between population and productivity by showing the relative contribution of coral population and calcification rate when the adapted temperature is too wide, is just right, or is too narrow. The first column shows how when the adapted range is too large the histogram of the temperatures falls entirely under the transient temperature curve. Although no bleaching occurs so the population is the greatest of the three, its possible calcification rate is the lowest due to the penalty imposed by the large adapted range. The third column show when the adapted range is too small a significant fraction of the histogram of temperatures falls above  $T_{hi}$ . Although the maximum possible rate of calcification is higher than the optimal or wide specialisation scenarios, the high frequency and intensity of bleaching reduces the healthy population that in turn reduces the net calcification.

The optimal temperature range strikes the balance between the risk of bleaching and net calcification rate, resulting in the highest realised growth rate of the three potential thermal specialisation scenarios (Fig. 6). Some bleaching will occur, however thermal tolerance has been optimized to maximise the balance between potential total calcification and bleaching frequency. This fits nicely with the observations and understanding of bleaching in corals. The widely made observation that corals are 1–2 °C from bleaching would appear to be a fragile choice for organism. However, in the framework of our model this seeming risk choice makes sense; corals have adapted to their local temperature regime to maximise both their productivity and population.

Therefore, by maximising the total calcification rate the adapted range ( $T_{lo}$  and  $T_{hi}$ ) can be determined on a per location basis from a record of historical temperatures. This is very powerful tool allows this model to be applied globally to either observational

## BGD

11, 187–249, 2014

### Modeling coral calcification

C. Evenhuis et al.

Title Page

Abstract

Introduction

Conclusions

References

Tables

Figures



Back

Close

Full Screen / Esc

Printer-friendly Version

Interactive Discussion



records or to climate model output. This leaves the species constant  $C_{sp}$  as the sole remaining “free parameter” in the model.

## 2.3 The thermal envelope ( $\beta$ )

The final term to be determined in our model is the thermal envelope, which is used to relate differences in productivity of corals between different locations. In the previous sections the absolute rate of calcification was not important as it was used only to determine the adapted temperature response. In this section an absolute value is put on the rate of calcification.

Determining a value for the rate of calcification is challenging, as there is a wide variation in measured calcification rates between different experimental protocols. Kleypas and Langdon (2006) identified seven experimental approaches for measuring calcification rate, with spatial scales ranging from individual corals to whole reef communities, and temporal scales from hours to millennia. Here we have used the large dataset of calcification rates for *Porites* compiled by Lough et al. (Lough and Barnes, 1997, 2000; Poulsen et al., 2006; Lough, 2008). This dataset allows the calcification rate of a single species (*Porites*) to be compared across 60 unique geographic locations (Shi et al., 2012; Scoffin et al., 1992; Poulsen et al., 2006; Lough, 2008; Fabricius et al., 2011; Edinger et al., 2000; Cooper et al., 2012).

The thermal envelope is characterised by examining how the rate of calcification varies between locations due to differences in the local temperatures. The increase in biological function with average temperature is a well-known phenomenon and is commonly modelled using the Boltzmann–Arrhenius curve. This Arrhenius equation can be viewed as an upper bound on the thermal efficiency of corals. The details of how this energy is used by a specific coral is determined by the adapted response  $\alpha$  and the species constant  $C_{sp}$ . To this point we have ignored the contribution to the to temperature from the thermal envelope by implicitly setting  $\beta = 1$ . By defining the thermal envelope so that is it 1 when the average temperature 300 K we can extended the model, which so far has only been applied to Hawaii and the Great Barrier Reef, to

## Modeling coral calcification

C. Evenhuis et al.

Title Page

Abstract

Introduction

Conclusions

References

Tables

Figures

◀

▶

◀

▶

Back

Close

Full Screen / Esc

Printer-friendly Version

Interactive Discussion



other locations. This is achieved by defining the thermal envelope as:

$$\beta(T_{\text{opt}}, E_a) = \exp \left[ \frac{E_a}{R \left( \frac{1}{300} - \frac{1}{T_{\text{opt}}} \right)} \right], \quad (8)$$

where  $E_a$  is the activation energy and  $R$  is the gas constant. Figure 7b shows the effect of changing the average temperature  $T_{\text{opt}}$  whilst the temperature range  $\Delta T$  is held constant.

However, problems arise if the thermal envelope is used with the adapted response from Eq. (7). From Eq. (7) it can be seen that growth rate at a given temperature is proportional to  $\Delta T^{-1}$ . By being inversely proportional to the adapted range the adapted response curve decreases too slowly when the temperature range is large and increases too quickly when the temperature range is small. The problem of slow decrease when the temperature range is large can be illustrated by considering how the thermal envelope and the adapted response curve behave as the upper threshold increases while keeping the lower threshold fixed. For the temperatures of interest the Arrhenius term can be approximated as an exponential, and by expressing  $T_{\text{opt}}$  in terms of  $T_{\text{lo}}$  and  $\Delta T$ , the increase from the thermal envelope is can be approximated as:

$$\beta(T_{\text{opt}}, E_a) \approx \exp \left[ \frac{E_a}{R \left( \frac{T_{\text{opt}} - 300}{300^2} \right)} \right] \propto \exp \left( \frac{E_a}{R} \frac{\Delta T}{300^2 \sqrt{3}} \right). \quad (9)$$

The problem is that the exponential increase in the thermal envelope outpaces the decrease from the normalisation term  $\Delta T^{-1}$ . Consequently, as the upper threshold is increased at some point the increase in thermal envelope is bigger than the penalty incurred for having a large adapted range. This means that when the calcification rate is maximised it is possible for  $T_{\text{hi}}$  to increase without bound. One way to address the runaway upper threshold would be to modify the thermal envelope to use, for example,

the extended Boltzmann Arrhenius equation (Dell et al., 2011). Alternately, limiting the size of the adapted range or increasing the penalty for having a large adapted range could also address the problem.

A similar problem arises when the temperature range is small. As the area under the adapted response curve is conserved the maximum rate (the rate at  $T_{opt}$ ) is proportional to  $\Delta T^{-1}$ , which results in clearly unrealistically behaviour when the adapted temperature range is small. As a thought experiment consider a coral that has adapted to three locations that have the same average temperature and temperature range of 10°C, 1°C and 0.1°C. If the adapted temperature curve is normalised the model would predict the 1°C and 0.1°C sites to have the 10 and 100 times the growth rate of the 10°C site. One would expect some increase in growth rate to occur as the range shrinks as a result of thermal specialisation, but for it to ultimately approach some limit. A solution would be to place limits on the minimum temperature range or to “roll-off” the normalisation factor to a constant as the temperature range decreases.

The most direct solution to the above two problems is to replace the normalisation term by an exponential. The exponential replacement is designed to decay faster than the thermal envelope and to match the behaviour of the normalisation term around 10°C. The updated version of the adapted response curve is now:

$$\alpha(T; T_{opt}, \Delta T) = \begin{cases} T > T_{lo} : \overset{\text{Cubic Polynomial}}{-(T - T_{lo}) \left( (T - T_{lo})^2 - \Delta T^2 \right)} 4 \times 10^{-4} \overset{\text{Normalisation}}{\exp[-0.33(\Delta T - 10)]} \\ T < T_{lo} : \underset{\text{Constant}}{-\alpha_{max}} \end{cases} \quad (10)$$

where:

$$T_{lo} = T_{opt} - \frac{1}{\sqrt{3}} \Delta T$$

$$T_{hi} = T_{lo} + \Delta T$$

Using the equation above the exponential normalisation factor can outpace the rise in the thermal envelope for activation energies up to  $500 \text{ kJ mol}^{-1}$ , which is well above the range of biochemical reactions.

Having established a mechanism to avoid the spurious high temperature runaway the calcification constant in Eq. (1), the normalisation correction  $\delta$  from Eq. (7) and the activation energy  $E_a$  in Eq. (8) are found by fitting the model to the observed calcification rates. For each location the adapted temperature range was determined by maximising the calcification rate over the historical period (1900–1970). The relative distribution of aragonite saturation state was estimated from GLODAP (Key et al., 2004) and WOA (Conkright et al., 2002). Given that the changes in calcification due to changes in ocean acidification are small over the historical period, a single (time invariant) value of aragonite was used in each location.

The average calcification rate over the historical period was calculated by minimising the residual between the calculated and observed calcification rates, shown in Fig. 8. From this the rates for the values of  $g_C = 0.038 \text{ g cm}^{-2} \text{ d}^{-1}$ ,  $\delta = 0.33$  and  $E_a = 50 \text{ kJ mol}^{-1}$  were determined. Interestingly, the magnitude of the calcification constant puts calcification processes on the same timescale as growth and reproduction. Similarly, the activation energy falls within the range that is observed for biological processes (Dell et al., 2011). The value  $\delta > 0$  reflects the inefficiency in the allocation of resources to small temperature ranges.

In the final section of the results a simplified version of the model is constructed that is used to show the linear relationship between calcification rate and average temperature observed by Lough and Barnes can emerge from the Arrhenius relationship, the penalty imposed on large adapted ranges, and from the correlation between average temperatures and temperature ranges.

**BGD**

11, 187–249, 2014

## Modeling coral calcification

C. Evenhuis et al.

Title Page

Abstract

Introduction

Conclusions

References

Tables

Figures

◀

▶

◀

▶

Back

Close

Full Screen / Esc

Printer-friendly Version

Interactive Discussion



### 3 Results and assessment

Having outlined the construction of the model in the previous section, here the model is assessed against three sets of experimental results that were not used in the construction of the model. The model was constructed starting with the smallest spatial and temporal scales (minutes, organism) and systematically built up to the largest (centuries, geographic). As no one single experiment is able to bridge these spatial and temporal timescales, we validate the model with a set of experiments that tests a subset of the components. In this way, although in isolation a single experiment assesses only part of the model, when taken in aggregate they demonstrate the overall performance and robustness of the model.

In the final section of the results a simplified version of the model is constructed that is used to show the linear relationship between calcification rate and average temperature observed by Lough and Barnes can emerge from the Arrhenius relationship, the penalty imposed on large adapted ranges, and from the correlation between average temperatures and temperature ranges.

#### 3.1 Aragonite, adapted response, local temperature range

The first assessment of our model compares the simulated calcification rates with those reported by Erez et al. (2011) (Fig. 11; originally reported in Schneider and Erez, 2006). In this experiment calcification of the coral *Acropora eurystoma* was measured as a function of aragonite saturation state and temperature. The comparison between the experimental results and the model output is shown in Fig. 9 this assesses the expression used for calcification (Eq. 1) and links adapted temperature response to the local climate.

The experimental data in the left hand panel of Fig. 9 clearly displays the linear response to aragonite saturation. In order to achieve good fit with the linear response a constant dissolution rate was added to the experimental results, which enables the measured gross calcification rate used in the model to be inferred from the measured

BGD

11, 187–249, 2014

## Modeling coral calcification

C. Evenhuis et al.

Title Page

Abstract

Introduction

Conclusions

References

Tables

Figures

⏪

⏩

◀

▶

Back

Close

Full Screen / Esc

Printer-friendly Version

Interactive Discussion



gross calcification rates from the reported values. The calcification rates were measured at three temperatures and show that optimal calcification rates were achieved at 24 °C. The model highlights the strong dependence of calcification on temperature, as calcification rates across a range of  $\Omega_{\text{arg}}$  are reduced at temperatures above (29 °C) and below (21 °C) the optimal temperature ( $\sim 25$  °C).

The right hand panel of Fig. 9 demonstrates how the maximum observed calcification rates are linked to the local or adapted temperature range. The temperatures thresholds that define the adapted response curve were found by optimizing the calcification rate, as described in Sect. 2.2.7, and is plotted over the histogram of the historical SSTs as shown in Fig. 9. Maximum calcification is observed at 25 °C, 3 °C below the local seasonal maximum SST, and 5 °C above the local seasonal minimum SST. The dashed lines connecting the left and right panels of Fig. 9 shows the dependence of calcification rate on both the aragonite saturation state and temperature and emphasizes that temperature is the dominant driving enhancing calcification across a range of  $\Omega_{\text{arg}}$ .

### 3.2 Population changes, species, optimizing to local climate

The second assessment of our model utilises the observations of the 1998 bleaching event on the GBR reported by (Baird and Marshall, 2002). Specifically, this work reported how four different species of coral bleached and recovered over subsequent months. The translations of the states used to classify the condition of the coral from the observations to the 5 states used in the model are given Table 3.

The model was initialised with 100 % healthy coral, and in situ temperatures used for 1998 (available from the AIMS website: [www.aims.gov.au](http://www.aims.gov.au)). Figure 10 shows good agreement between the observations and model and provides a test of the ability of the model to reproduce the observed response. The values for the species constants were determined by matching the model output to the observations and are in good agreement with data from Sect. 2.5 (Fig. 5), and demonstrate the importance of species composition in modulating bleaching and recovery within a coral reef community.

**BGD**

11, 187–249, 2014

## Modeling coral calcification

C. Evenhuis et al.

Title Page

Abstract

Introduction

Conclusions

References

Tables

Figures

◀

▶

◀

▶

Back

Close

Full Screen / Esc

Printer-friendly Version

Interactive Discussion



## Modeling coral calcification

C. Evenhuis et al.

Title Page

Abstract

Introduction

Conclusions

References

Tables

Figures

◀

▶

◀

▶

Back

Close

Full Screen / Esc

Printer-friendly Version

Interactive Discussion



The third assessment of the model uses the reciprocal transplant experiment of Howells et al. (2013) which highlights the importance of the adapted range. This experiment monitored the health of corals that were exchanged between reefs on the central and southern GBR. Corals relocated from the southern to the central site experienced temperatures above their adapted range and bleached due to heat stress, whilst corals transferred from the central to the southern site experienced temperatures below their adapted range and bleached due to cold stress.

The two locations, Nelly Bay (central GBR) and Miall Island (southern GBR), have significantly different climatologies, which is reflected in their respective adapted ranges.

Table 4 shows the thermal thresholds for the two locations, calculated by four methods using two SST time series (the NOAA AVHRR product and in situ temperature logger records). The first approach estimates the adapted range by calculating extreme percentiles of the SST distribution – in this case the percentiles correspond to 1-in-3 year temperature extremes. The second adapts a common bleaching metric (Maximum Monthly Mean plus variance). The third employs the optimisation procedure outlined in section 0 that maximises the calcification rate over the historical period. Finally, in the empirical approach the upper and lower thresholds were manually adjusted to reproduce the experimental observations. The spread in values highlights some of the difficulties in estimating thermal thresholds which impact on the severity and timing of coral bleaching and recovery.

There are a number of challenges when a coral's adapted range is calculated from an SST product and then compared to bleaching observations. Firstly, the low spatial resolution ( $0.25^\circ$  for NOAA (Reynolds et al., 2007),  $1^\circ$  for HADISST, Rayner et al., 2003) means that temperature fluctuations at the scale of the reef are averaged out, so in general the thermal variability is underestimated. Secondly, hydrodynamic processes that take place reef can lead to systematic differences that are not resolved by SST products and which vary throughout the year. For example, the local trapping and flushing of the water on a reef driven by tides and winds can result in large system-

atic variations in the water temperatures that are not resolved by the SST products. Clearly in situ recordings of SSTs can capture the reef-scale temperature more accurately, however they are not widely available, often covering shorter periods, and may be subject to data integrity problems. To accurately estimate thermal thresholds the temperatures are needed over a long time period, which unfortunately rules out in situ measurements in most cases.

Despite the limitations in estimating the adapted range, Table 4 shows good agreement between different approaches and the two temperature records; and that despite all of differences in techniques the upper and lower thermal thresholds differ by  $\sim 1.5^\circ\text{C}$  between the central and southern GBR sites. Overall the bleaching and recovery response is well captured in Figure 11, with the exception of the central-to-central transplant that was strongly influenced by a large flooding event that occurred in this region, resulting in total mortality. Flooding impacts coral in a number of ways, including increased nutrient input, and changes in organic matter and freshening. At present stochastic events such as flooding are not represented in our model.

### 3.3 Interpreting the Lough & Barnes relationship

Rates of coral growth (linear extension and calcification) are strongly linked to annual average SST. *Porites* extension increases by  $\sim 3\text{ mm yr}^{-1}$  for every  $1^\circ\text{C}$  increase in average SST (Lough and Barnes, 2000). Since this relationship was observed for GBR *Porites* by (Lough and Barnes, 2000) it has been reaffirmed for many other regions by numerous other studies (Poulsen et al., 2006; Lough, 2008). This linear relationship, hereafter referred to as L&B, has some surprising features. Firstly, it predicts the rate of calcification falls to zero when the average annual SST is  $\sim 22^\circ\text{C}$ . Secondly, it is difficult to reconcile the predicted increased temperature response with the typical temperature response of coral (i.e. the adapted response curve). Finally, as there is no single biological response that is expected to have such a linear response (as seen in L&B), it is likely that it arises from the interaction of several processes.

**BGD**

11, 187–249, 2014

## Modeling coral calcification

C. Evenhuis et al.

Title Page

Abstract

Introduction

Conclusions

References

Tables

Figures

◀

▶

◀

▶

Back

Close

Full Screen / Esc

Printer-friendly Version

Interactive Discussion



## Modeling coral calcification

C. Evenhuis et al.

Title Page

Abstract

Introduction

Conclusions

References

Tables

Figures

◀

▶

◀

▶

Back

Close

Full Screen / Esc

Printer-friendly Version

Interactive Discussion



In this section we demonstrate how our model can be used to explain how the linear L&B calcification relationship to annual average SST emerges from the adapted temperature range as calcification rates have been optimised to reach a maximum rate close to annual average SST's (Fig. 9b). Here we derive a simplified model (SM) from our model by applying a number of approximations to Eq. (1), so that only the Arrhenius term and the normalization term that rewards thermal specialisation remain. The resulting relationship describes the calcification rate in terms of only the adapted temperature range  $[T_{lo}, T_{hi}]$ .

To derive the SM we first assume that over longer historical periods the effect of bleaching events average out so the healthy population is approximately constant, i.e.  $P_H = 1$ . Similarly, the species constant is set so that  $C_{sp} = 1$  and the aragonite saturation state and daily insolation is set to a fixed value. Rather than finding the adapted range by optimising the calcification rate, it is assumed that the adapted range corresponds to the 1st and 99th percentiles of the temperature distribution. The final step is to assume that the temperatures are uniformly distributed, i.e. all temperatures between  $T_{lo}$  and  $T_{hi}$  are equally likely to occur. This allows the average of the adapted response over the days of the year to be replaced by an integral over temperature. The adapted response curve was constructed so that the integral over the temperature gives  $\Delta T^\delta$ , and the assumption of uniformly distribution temperatures contributes  $\Delta T^{-1}$  to give:

$$\dot{G}_{ave} = A \exp \left[ \frac{E_a}{R} \left( \frac{1}{T_{ave}} - \frac{1}{300} \right) \right] \frac{1}{\Delta T^{1-\delta}} \quad (11)$$

where  $\Delta T = T_{99} - T_{01}$ ,  $E_a$  is the activation energy,  $\delta$  is the normalisation factor that rewards thermal specialisation, and  $A$  is a constant. Equation (10) has a very simple interpretation, the calcification rate is given by an Arrhenius curve that depends on the average temperature, and which is modulated by the temperature range.

We stress that the normalisation  $\delta$  in Eq. (11) corresponds to a different value of  $\delta$  from that in the full model. The assumptions used to derive Eq. (11) cause the penalty

## Modeling coral calcification

C. Evenhuis et al.

Title Page

Abstract

Introduction

Conclusions

References

Tables

Figures

◀

▶

◀

▶

Back

Close

Full Screen / Esc

Printer-friendly Version

Interactive Discussion



for being thermal generalist to increase for two reasons. Firstly, at high latitude locations the temperature distribution is bimodal and has a distinct summer-time peak close to  $T_{hi}$  and the winter-time peak close to  $T_{lo}$ . The assumption that the temperatures are uniformly distributed results in the average of the adapted response curve being over-

5 estimated at high latitudes. Secondly, approximating the daily insolation as  $\bar{Q}^{\text{day}} = 1$  also leads to overestimation at high latitude locations. These two sources of overestimation at high latitudes are addressed by recognising that the temperature range is correlated with latitude and increasing the penalty on  $\Delta T$  (i.e. reducing  $\delta$ ).

The fit of the SM (Eq. 11) to the data of L&B is shown in Fig. 12b. This is the same calcification rate data used in Fig. 8 from a single species (*Porites*) across 60 unique geographic locations (Shi et al., 2012; Scoffin et al., 1992; Poulsen et al., 2006; Lough, 2008; Fabricius et al., 2011; Edinger et al., 2000; Cooper et al., 2012; Grigg, 1981). The values of the were determined to be  $A = 1.8$ ,  $E_a = 50 \text{ kJ mol}^{-1}$  and  $\delta = 0$ . The values of the activation energy in the simplified and full versions of the model are close (45 vs. 50) and the value of  $\delta$  is reduced, as anticipated (0.0 vs. 0.33). The goodness of fit can be gauged by comparing the data points which are coloured by their temperature range to the family of Arrhenius curves obtained by setting  $\Delta T$  to 3, 4, 6, 8, and 15 °C.

The SM allows us to show how the linear relationship of L&B, and its spread, emerges from the relationship between the average temperature and the temperature range, the Arrhenius factor and the thermal specialization reward. The family of Arrhenius curves in Fig. 12b maps the area of possible calcification rates. By examining how average temperature and range co-vary we can narrow down the possibilities and demonstrate how the L&B relationship arises. Figure 12a plots the average and range of SST from the 0.25° NOAA SST (Reynolds et al., 2007) for each location. Most of the average-range data in Fig. 12a falls into a typical-temperature area (shaded grey) that is defined by fitting three average-range relationships. When the average-range relationships are substituted into Eq. (11) the typical-temperature area from Fig. 12a is flipped and distorted into the typical-calcification area in Fig. 12b. The final step to link the SM to the L&B relationship is to fit a regression line through the typical-calcification

## Modeling coral calcification

C. Evenhuis et al.

Title Page

Abstract

Introduction

Conclusions

References

Tables

Figures

◀

▶

◀

▶

Back

Close

Full Screen / Esc

Printer-friendly Version

Interactive Discussion



area. As the L&B relationship neatly bisects the typical-calcification area the lines are very close to one another, which illustrates how the L&B relationship emerges from two basic biological relationships. In addition, our SM also allows the spread of calcification rates about the L&B relationship to be understood. For example the spread of points above the line around the average temperature  $26^{\circ}\text{C}$  can be explained by the relationship between temperature range and averages in different water masses.

Outliers from the L&B relationship can be explained by having atypical temperature ranges. For example, the calcification rate for Houtman Albrous Reef (Cooper et al., 2012), which is anomalously high if the L&B relationship is used, can be understood in the SM as arising from having a lower temperature range than is typical for the average temperature. Similarly, the Milne Bay calcification rates of Fabricius et al. (2011) lie below the L&B relationship as it is growing in a region that has a larger temperature range than expected for the average temperature.

The clear outliers from the SM are the results of (Poulsen et al., 2006) from the Arabian Gulf, which stand out as the four red data points in Fig. 12b. Contrary to the observed calcification rate, Eq. (11) predicts a very low calcification rate due to the large temperature range. This large disagreement may in part be due to neglecting the aragonite saturation state (which is high in the Arabian Gulf), or it may simply suggest that the extreme conditions have resulted in a very different biological response in these corals. Nevertheless, this suggests SSTs is not likely the dominant driver of calcification for corals in the Arabian Gulf.

When comparing the goodness of the two fits we see that L&B has a better fit despite the SM employing an additional parameter. By this metric the L&B relationship is a better model as it uses less parameters. The use and dependence of the SM on the temperature range, which has a much higher uncertainty than the average temperature, likely contributes to the reduced ability of the SM to completely recreate the L&B relationship. The uncertainty in the range can be illustrated by comparing the averages and ranges calculated from the  $0.25^{\circ}$  NOAA SST (Reynolds et al., 2007) with in situ observations from the AIMS temperature loggers for 24 locations on the GBR. The

NOAA SST slightly underestimates the value of the average and the range by  $\sim 0.2^{\circ}\text{C}$ , which is consistent with the effects of spatial averaging. How the average and ranges from the NOAA product vary from the in situ observations is distinctly different. The spread of the differences of the average is  $0.9^{\circ}\text{C}$ , while the spread in the difference range is  $1.7^{\circ}\text{C}$ . That is, when the NOAA SST product is used in place of in situ data the uncertainty in the temperature ranges has roughly doubled that of the average temperatures. The larger uncertainty in the range arises from reef-scale processes that are not resolved by the NOAA product. Therefore, using the temperature ranges the SM significantly increases the size of random errors, which in turn reduces the goodness of fit.

## 4 Discussion

The new model presented here can be viewed as extending upon and bringing together the existing models of the coral growth response to ocean warming and acidification Silverman et al. (2009) and Buddemeier et al. (2008) that have different foci and limitations. The approach of Buddemeier et al. (2008) is a high-resolution model in time, focusing on specific locations and species while Silverman et al. (2009) are motivated by the large-scale trends and take a global view. Our new model brings together the low-level detail of species responses and adaptation to local environments that underpins the COMBO model (Buddemeier et al., 2008), by comparing across species and locations it distills the trends and patterns that emerge on a global scale. The result is a model that captures fine details in response of corals at the same time as extracting transferable relationships, all whilst aiming to have as few “free-parameters” possible.

In the modeling approach of Silverman et al. (2009) the (gross) calcification rate is proportional to the area of the reef, the proportion of the reef that is calcifying and depends on the temperature and aragonite saturation state. The aragonite saturation state, in turn, is proportional to the inorganic precipitation rate, which includes a complex dependence on temperature. Specifically, the temperature dependence is mod-

**BGD**

11, 187–249, 2014

## Modeling coral calcification

C. Evenhuis et al.

Title Page

Abstract

Introduction

Conclusions

References

Tables

Figures

◀

▶

◀

▶

Back

Close

Full Screen / Esc

Printer-friendly Version

Interactive Discussion



eled by a Gaussian curve centered on an optimal temperature with the width of the curve depending on the aragonite saturation state. However, relative to our model, the impact of temperature on calcification is quite simplistic; the fraction of calcifying corals is reduced by 50 % if the maximum monthly SST increases by 1 °C. Our model extends on the work of Silverman by including high frequency SST information and discriminating between individual species we are able to more realistically describe bleaching events.

The COMBO model of Buddemeier et al. (2008) also shares many similarities with the model presented in this work. For example the aragonite dependence is similar to our model, in that a range of responses from flat to a linear decrease can be modeled. In COMBO the temperature dependence of calcification is also modeled as cubic polynomial, however this needs to be parameterized for each location and potentially for each species. Our model extends COMBO by allowing the temperature to be applied globally by identifying transferable terms, thereby avoiding a re-parameterization for each new location. Another important point of difference is in how this temperature response impacts the coral. In the COMBO model bleaching is calculating Degrees Heating Weeks (DHW) and relating this to a percentage of coral mortality (see Fig. 3 of (Hoeke et al., 2011)). For a moderate increase in complexity, our new for a model, moves beyond the two (binary) corals states offered by DHW (healthy or bleached) to four states (healthy, pale, bleached, dead) that are used link growth and stress processes in coral. In doing this the thermal thresholds emerge naturally as a consequence of the trade-off between growth and stress, replacing the statistic heuristics such as Mean Monthly Maximum that are used in a DHW calculation. It also moves away from the need to rely on a fixed recovery period e.g. (Donner et al., 2005), by explicitly modeling the recovery process as its dependence on temperature. The connection between our new model and DHW is clear if Eq. (2) is discretized to give a difference equation. This difference equation simply sums the temperature over the threshold  $T_{hi}$ , and is clearly closely related to the formula for calculating DHW.

**BGD**

11, 187–249, 2014

## Modeling coral calcification

C. Evenhuis et al.

Title Page

Abstract

Introduction

Conclusions

References

Tables

Figures

◀

▶

◀

▶

Back

Close

Full Screen / Esc

Printer-friendly Version

Interactive Discussion



## Modeling coral calcification

C. Evenhuis et al.

Title Page

Abstract

Introduction

Conclusions

References

Tables

Figures

◀

▶

◀

▶

Back

Close

Full Screen / Esc

Printer-friendly Version

Interactive Discussion



In this work the temperature response is key to understanding how corals grow and bleach due to temperature stress. The adapted response function that captures this temperature dependence is an example of a *reaction norm* – a response of an organism that varies continuously with an environmental variable (Stearns, 1998). Reaction norms describe how organisms with the same genetics (genotype) are able to express a variety of responses depending on its environment (phenotype). By realising that the adapted response is a *reaction norm* the connections between multiple traits can be made. All of the traits in the model share a common temperature dependence reflecting their dependence on the symbiosis, and the different bleaching sensitivities between coral species manifest as traits that are either up regulated or down regulated in a correlated fashion by the species parameter ( $C_{sp}$ ) that was defined based upon previous bleaching observations.

The model uses the normalization of the adapted response to reward thermal specialization, which is an approach that other researchers have linked to the trade-off between being a thermal generalist or specialist (Gilchrist, 1995). The correlated up- and down- regulation of growth and thermal protection processes, that are controlled by the species parameter  $C_{sp}$ , can also be viewed in terms of resource allocation. This trade-off is analogous to the  $\kappa$ -rule in *Dynamic Energy Budget* theory that determines the allocation of energy between growth and reproduction (Nisbet et al., 2000). The extremes of this trade-off spectrum correspond to two distinct strategies for coping with thermal stress: a growth and a resilience strategy. Small values of the species parameter correspond to slow-growing species that can survive bleaching episodes, whilst large values correspond to fast-growing species that can regrow quickly after a disturbance. The relative merits of these two thermal resilience strategies under global warming scenarios remains unclear and is an active area of current research. One likely outcome if catastrophic bleaching events become more frequent, is that community composition will favor the slow growing, tolerant species ( $C_{sp} < 0.5$ , Fig. 5) as the recovery time will be insufficient between stress events to promote recovery of the faster growing, sensitive species ( $C_{sp} > 0.5$ , Fig. 5).

When the simulated coral calcification rate was compared with the observed calcification rate (Fig. 8), a few points lay off the line indicating that the model over and underestimates the observed rate in some locations. This comparison relies on the temperatures from relatively coarse resolution products ( $0.25^\circ \times 0.25^\circ$ ), whilst the observed calcification rates record the high-resolution in situ temperature. If the SST product underestimates the range of temperatures the model will predict artificially high calcification rates and the point will lie above the line in Fig. 8. Likewise, overestimation of temperature range leads to underestimation of calcification rates. There can be large differences between in situ recorded temperature and the SST products, particularly in the coastal environment (Lima and Wethey, 2012). For example, many sites for which the model underestimates the calcification rate e.g. Poulsen et al. (2006) are close to land and therefore maybe influenced by local warming that increases the temperature range. Furthermore, sites close to land are more likely to impacted by high nutrient levels. As these differences are often not systematic there is no simple way to correct for these differences. Factors not included in the model that are known to reduce calcification could account for model overestimating at some locations. For example, pollution (Edinger et al., 2000), differences in PAR (photosynthetically available radiation) due organic matter in the water column or cloud properties, and “top down” ecosystem pressures all could be responsible for reductions in calcification rate. Nevertheless, the model is able to capture many of the observed responses using only low-resolution temperature records and a qualitative measure of the species. We believe that the largest improvements in the model would come from higher resolution temperature records.

It is clear from the wide range of temperature regimes that corals have adapted to adapt to local conditions but the rate at which this adaptation takes place is assumed to be too slow to keep pace with projected warming scenarios (Hoegh-Guldberg et al., 2007). See Coles and Brown (2003) for a review of the possible routes of adaption. The fastest of these are phenotypic processes that operate on monthly to yearly time scales, and include enzymatic and physiological responses and shuffling or exchange

## BGD

11, 187–249, 2014

### Modeling coral calcification

C. Evenhuis et al.

Title Page

Abstract

Introduction

Conclusions

References

Tables

Figures

◀

▶

◀

▶

Back

Close

Full Screen / Esc

Printer-friendly Version

Interactive Discussion



of zooxanthellae (ie. adaptive bleaching hypothesis (Kinzie et al., 2001; Jones, 2008). On longer timescales, from decades to centuries, genetic changes are effected by selection pressure and evolution. The underlying mechanisms, the range or plasticity of this change, and the rate of these adaption processes are, as yet, not fully understood, remaining an ongoing area of research. Adaption on annual to decadal timescales is of greatest relevance to the medium term climate projections of coral health. In our model we do not explicitly consider adaptation, and we note that in applying this model, particularly over longer periods that the potential for adaptation needs to be considered.

If the only the inorganic solution equilibrium of Aragonite is considered coral reefs will not dissolve until  $\Omega < 1$ . However, there are additional dissolution processes that occur on reefs, such as bio-erosion and mechanical damage (Silverman et al., 2009; Andersson and Gledhill, 2013), so it is expected that net dissolution for some value of  $\Omega > 1$ . Dissolution terms are commonly employed when interpreting experimental results and dissolution rates have been measured in a range of experimental setups and reef locations (see for example Table 3.2 in Kleypas et al., 2006; and Table 1 in Andersson and Gledhill, 2013). The rates of dissolution vary with habitat makeup and ecosystem composition and remain an active and important area of research. Here we have only calculated the gross calcification term, and as such if this model were to be applied over longer scales or used to for projections into the future, clearly a dissolution term must be included.

Coral bleaching and ocean acidification have been identified as two of the key stressors for coral reefs in a warming world. However, corals face many additional pressures such as changes in nutrient supply and light, riverine input, storm damage, disease and human pressures (Burke et al., 2011). All of these can impact on coral calcification rates and reduce the ability of a coral to buffer the impacts of increasing temperatures and thereby reduce its resilience to environmental stress (Edinger et al., 2000). As many of these stressors are stochastic in nature it is impossible to explicitly model them and, hence, the response of corals. However, the model we present here provides a solid foundation and allows us to explore how these processes may impact

**BGD**

11, 187–249, 2014

## Modeling coral calcification

C. Evenhuis et al.

Title Page

Abstract

Introduction

Conclusions

References

Tables

Figures

⏪

⏩

◀

▶

Back

Close

Full Screen / Esc

Printer-friendly Version

Interactive Discussion



corals and how these pressures may interact with ocean acidification and increasing ocean temperatures.

## 5 Conclusions

Corals reefs are diverse ecosystems that support about 25 % of the total global biodiversity. Rising CO<sub>2</sub> levels in the atmosphere taken up and sequestered by the ocean are driving the observed increases in sea surface temperature and ocean acidification. While these are not the only pressures facing corals, they do represent two key stressors. In order to project how coral reefs may respond in the future, it is essential to understand the factors that impact the health of corals and their calcification rates.

Here we present a new model that uses temperature and carbonate chemistry to describe the response of coral calcification rates as an indicator of health. By synthesising published observational studies we link the rates of growth, recovery and calcification to temperature stress induced bleaching and mortality, which enables the changes in coral health and population to be explicitly modelled. Our work highlights the importance of annual temperature range, not just the upper temperature threshold, in determining the bleaching sensitivity and annual physiological performance of individual corals.

This new model draws on observations of corals from different locations and from different taxa to identify general, transferable relationships that relate the rates of growth, bleaching and calcification. The model is underpinned by four key principles; the Arrhenius equation (enhancement of biological and chemical reactions with increasing temperature), thermal specialisation, resource allocation trade-offs, and adaption to local environment. These general relationships allow the model to be constructed from a range of experimental and observational data and to minimize the number of “free parameters”.

We assessed the different characteristics of this model against independent data and show that the model captures the observed response of corals in various habitats and

**BGD**

11, 187–249, 2014

## Modeling coral calcification

C. Evenhuis et al.

Title Page

Abstract

Introduction

Conclusions

References

Tables

Figures

◀

▶

◀

▶

Back

Close

Full Screen / Esc

Printer-friendly Version

Interactive Discussion



## Modeling coral calcification

C. Evenhuis et al.

Title Page

Abstract

Introduction

Conclusions

References

Tables

Figures

⏪

⏩

◀

▶

Back

Close

Full Screen / Esc

Printer-friendly Version

Interactive Discussion



5 locations. With the exception of corals very close to land, where the ability of the model to simulate the response of observed calcification is limited, potentially due to local influences, not included in this model, such as warming, nutrient supply, hydrodynamics and changes in light level, the model does a very good job in reproducing observed calcification rates. As a consequence, the result is a robust, transferable model that is simple enough to be applied at many different temporal and spatial scales. Furthermore, this model provides a solid basis on which to build in additional complexity as needed or desired.

10 We show that, by simplifying our model, the observed linear response in global average calcification rates to average annual temperatures (Lough and Barnes, 2000) can be explained since coral growth rates have been optimized to maximize calcification rates at mid-range annual temperatures and close to the annual average SST. Further, this simplified model provides important new insights into the factors that determine calcification rates and gives a framework for understanding the observed distribution of calcification rates. Our results suggest that, despite the implicit complexity of the coral reef environment, a simple model based on temperature, carbonate chemistry and previous observations of species-specific responses can reproduce much of the observed coral response. Finally, our work highlights the importance of unifying the temperature and ocean acidification responses, and developing long-term in situ measurements of temperature, carbonate chemistry and coral health.

25 *Acknowledgements.* The authors wish to thank Qi Shi for make his original calcification data available. C. E. and A. L. were supported by the Pacific-Australia Climate Change Science and Adaptation Planning Program funded by AusAID in collaboration with the Department of the Environment, and delivered by the Bureau of Meteorology and the Commonwealth Scientific and Industrial Research Organisation. N. C. and J. M. L. acknowledge support from the Australian Institute of Marine Science and Australian Research Council Super Science Fellowships.

## References

- Adjeroud, M., Michonneau, F., Edmunds, P. J., Chancerelle, Y., Loma, T. L., Penin, L., Thibaut, L., Vidal-Dupiol, J., Salvat, B., and Galzin, R.: Recurrent disturbances, recovery trajectories, and resilience of coral assemblages on a South Central Pacific reef, *Coral Reefs*, 28, 775–780, doi:10.1007/s00338-009-0515-7, 2009.
- Al-Horani, F. A.: Effects of changing seawater temperature on photosynthesis and calcification in the scleractinian coral *Galaxea fascicularis*, measured with O<sub>2</sub>, Ca<sup>2+</sup> and pH microsensors, *Sci. Mar.*, 69, 347–354, 2005.
- Albright, R., Mason, B., and Langdon, C.: Effect of aragonite saturation state on settlement and post-settlement growth of *Porites astreoides* larvae, *Coral Reefs*, 27, 485–490, doi:10.1007/s00338-008-0392-5, 2008.
- Allemand, D., Tambutté, É., Zoccola, D., and Tambutté, S.: Coral calcification, *Cells to Reefs*, 119–150, doi:10.1007/978-94-007-0114-4\_9, 2011.
- Andersson, A. J. and Gledhill, D.: Ocean acidification and coral reefs: effects on breakdown, dissolution, and net ecosystem calcification, *Ann. Rev. Mar. Sci.*, 5, 321–348, doi:10.1146/Annurev-Marine-121211-172241, 2013.
- Andersson, A. J., Kuffner, I. B., Mackenzie, F. T., Jokiel, P. L., Rodgers, K. S., and Tan, A.: Net Loss of CaCO<sub>3</sub> from a subtropical calcifying community due to seawater acidification: mesocosm-scale experimental evidence, *Biogeosciences*, 6, 1811–1823, doi:10.5194/bg-6-1811-2009, 2009.
- Anthony, K. R. N., Hoogenboom, M. O., Maynard, J. A., Grottoli, A. G., and Middlebrook, R.: Energetics approach to predicting mortality risk from environmental stress: a case study of coral bleaching, *Funct. Ecol.*, 23, 539–550, doi:10.1111/j.1365-2435.2008.01531.x, 2009.
- Baird, A. H. and Marshall, P. A.: Mortality, growth and reproduction in scleractinian corals following bleaching on the Great Barrier Reef, *Mar. Ecol.-Prog. Ser.*, 237, 133–141, doi:10.3354/Meps237133, 2002.
- Baird, A. H., Bhagooli, R., Ralph, P. J., and Takahashi, S.: Coral bleaching: the role of the host, *Trends Ecol. Evol.*, 24, 16–20, doi:10.1016/j.tree.2008.09.005, 2009.
- Baker, A. C.: Flexibility and specificity in coral-algal symbiosis: Diversity, ecology, and biogeography of Symbiodinium, *Annu. Rev. Ecol. Evol. S.*, 34, 661–689, doi:10.1146/Annurev.Ecolsys.34.011802.132417, 2003.

BGD

11, 187–249, 2014

### Modeling coral calcification

C. Evenhuis et al.

Title Page

Abstract

Introduction

Conclusions

References

Tables

Figures

◀

▶

◀

▶

Back

Close

Full Screen / Esc

Printer-friendly Version

Interactive Discussion



## Modeling coral calcification

C. Evenhuis et al.

Title Page

Abstract

Introduction

Conclusions

References

Tables

Figures

◀

▶

◀

▶

Back

Close

Full Screen / Esc

Printer-friendly Version

Interactive Discussion



Baker, A. C., Glynn, P. W., and Riegl, B.: Climate change and coral reef bleaching: An ecological assessment of long-term impacts, recovery trends and future outlook, *Estuar. Coast. Shelf S.*, 80, 435–471, doi:10.1016/j.ecss.2008.09.003, 2008.

Baker, P. A. and Weber, J. N.: Coral growth rate: variation with depth, *Phys. Earth Planet. In.*, 10, 135–139, 1975.

Berkelmans, R., De'ath, G., Kininmonth, S., and Skirving, W. J.: A comparison of the 1998 and 2002 coral bleaching events on the Great Barrier Reef: spatial correlation, patterns, and predictions, *Coral Reefs*, 23, 74–83, doi:10.1007/s00338-003-0353-y, 2004.

Broecker, W. S., Langdon, C., Takahashi, T., and Peng, T.-H.: Factors controlling the rate of  $\text{CaCO}_3$  precipitation on Great Bahama Bank, *Global Biogeochem. Cy.*, 15, 589, doi:10.1029/2000gb001350, 2001.

Brown, B. E. and Suharsono: Damage and recovery of coral reefs affected by El-Nino related seawater warming in the thousand islands, Indonesia, *Coral Reefs*, 8, 163–170, doi:10.1007/Bf00265007, 1990.

Brown, J. H., Gillooly, J. F., Allen, A. P., Savage, V. M., and West, G. B.: Toward a metabolic theory of ecology, *Ecology*, 85, 1711, 2004.

Buddemeier, R. W., Jokiel, P. L., Zimmerman, K. M., Lane, D. R., Carey, J. M., Bohling, G. C., and Martinich, J. A.: A modeling tool to evaluate regional coral reef responses to changes in climate and ocean chemistry, *Limnol. Oceanogr.-Meth.*, 6, 395–411, 2008.

Burke, L., Reyntar, K., Spalding, M., and Perry, A.: *Reefs at Risk Revisited*, World Resources Institute, Washington DC, USA, 2011.

Cantin, N. E., Cohen, A. L., Karnauskas, K. B., Tarrant, A. M., and McCorkle, D. C.: Ocean warming slows coral growth in the central Red Sea, *Science*, 329, 322–325, doi:10.1126/science.1190182, 2010.

Carilli, J. E., Norris, R. D., Black, B. A., Walsh, S. M., and McField, M.: Local stressors reduce coral resilience to bleaching, *PLoS ONE*, 4, 7, doi:10.1371/journal.pone.0006324, 2009.

Castillo, K. D., Ries, J. B., Weiss, J. M., and Lima, F. P.: Decline of forereef corals in response to recent warming linked to history of thermal exposure, *Nat. Clim. Change*, 2, 756–760, doi:10.1038/nclimate1577, 2012.

Ceccarelli, D. M., Richards, Z. T., Pratchett, M. S., and Cvitanovic, C.: Rapid increase in coral cover on an isolated coral reef, the Ashmore Reef National Nature Reserve, north-western Australia, *Mar. Freshwater Res.*, 62, 1214, doi:10.1071/mf11013, 2011.

## Modeling coral calcification

C. Evenhuis et al.

Title Page

Abstract

Introduction

Conclusions

References

Tables

Figures

◀

▶

◀

▶

Back

Close

Full Screen / Esc

Printer-friendly Version

Interactive Discussion



- Chan, N. C. S. and Connolly, S. R.: Sensitivity of coral calcification to ocean acidification: a meta-analysis, *Glob. Change Biol.*, 19, 282–290, doi:10.1111/Gcb.12011, 2013.
- Coles, S. L. and Brown, B. E.: Coral bleaching – capacity for acclimatization and adaptation, *Adv. Mar. Biol.*, 46, 183–223, doi:10.1016/S0065-2881(03)46004-5, 2003.
- 5 Coles, S. L. and Brown, E. K.: Twenty-five years of change in coral coverage on a hurricane impacted reef in Hawaii: the importance of recruitment, *Coral Reefs*, 26, 705–717, doi:10.1007/s00338-007-0257-3, 2007.
- Conkright, M. E., Locarnini, R. A., Garcia, H. E., O'Brien, T. D., Boyer, T. P., Stephens, C., and Antonov, J. I.: World OCEAN ATLAS 2001: Objective Analyses, Data Statistics and Figures, National Oceanographic Data Center, Silver Spring, MD, CD-ROM Documentation, 17, 2002.
- 10 Cooper, T. F., De'ath, G., Fabricius, K. E., and Lough, J. M.: Declining coral calcification in massive *Porites* in two nearshore regions of the northern Great Barrier Reef, *Glob. Change Biol.*, 14, 529–538, doi:10.1111/j.1365-2486.2007.01520.x, 2008.
- 15 Cooper, T. F., O'Leary, R. A., and Lough, J. M.: Growth of Western Australian Corals in the Anthropocene, *Science*, 335, 593–596, doi:10.1126/science.1214570, 2012.
- de Putron, S. J., McCorkle, D. C., Cohen, A. L., and Dillon, A. B.: The impact of seawater saturation state and bicarbonate ion concentration on calcification by new recruits of two Atlantic corals, *Coral Reefs*, 30, 321–328, doi:10.1007/S00338-010-0697-Z, 2011.
- 20 Dell, A. I., Pawar, S., and Savage, V. M.: Systematic variation in the temperature dependence of physiological and ecological traits, *P. Natl. Acad. Sci. USA*, 108, 10591–10596, doi:10.1073/pnas.1015178108, 2011.
- Diaz-Pulido, G., McCook, L. J., Dove, S., Berkelmans, R., Roff, G., Kline, D. I., Weeks, S., Evans, R. D., Williamson, D. H., and Hoegh-Guldberg, O.: Doom and boom on a resilient reef: climate change, algal overgrowth and coral recovery, *PLoS One*, 4, 4, e5239, doi:10.1371/journal.pone.0005239, 2009.
- 25 Doney, S. C., Fabry, V. J., Feely, R. A., and Kleypas, J. A.: Ocean acidification: the other CO<sub>2</sub> problem, *Annu. Rev. Mar. Sci.*, 1, 169–192, doi:10.1146/annurev.marine.010908.163834, 2009.
- 30 Donner, S. D., Skirving, W. J., Little, C. M., Oppenheimer, M., and Hoegh-Guldberg, O. V. E.: Global assessment of coral bleaching and required rates of adaptation under climate change, *Glob. Change Biol.*, 11, 2251–2265, doi:10.1111/j.1365-2486.2005.01073.x, 2005.

## Modeling coral calcification

C. Evenhuis et al.

Title Page

Abstract

Introduction

Conclusions

References

Tables

Figures

◀

▶

◀

▶

Back

Close

Full Screen / Esc

Printer-friendly Version

Interactive Discussion



- Donner, S. D.: An evaluation of the effect of recent temperature variability on the prediction of coral bleaching events, *Ecol. Appl.*, 21, 1718–1730, 2011.
- Edinger, E. N., Limmon, G. V., Jompa, J., Widjatmoko, W., Heikoop, J. M., and Risk, M. J.: Normal coral growth rates on dying reefs: are coral growth rates good indicators of reef health?, *Mar. Pollut. Bull.*, 40, 404–425, doi:10.1016/S0025-326x(99)00237-4, 2000.
- Edmunds, P. J.: The effect of sub-lethal increases in temperature on the growth and population trajectories of three scleractinian corals on the southern Great Barrier Reef, *Oecologia*, 146, 350–364, doi:10.1007/s00442-005-0210-5, 2005.
- Edmunds, P. J.: Differential Effects of High Temperature on the Respiration of Juvenile Caribbean Corals, *B. Mar. Sci.*, 83, 453–464, 2008.
- Erez, J., Reynaud, S., Silverman, J., Schneider, K., and Allemand, D.: Coral calcification under ocean acidification and global change, in *Coral Reefs: An Ecosystem in Transition*, edited by: Dubinsky, Z. and Stambler, N., 151–176, doi:10.1007/978-94-007-0114-4\_10, 2011.
- Fabricius, K. E., Langdon, C., Uthicke, S., Humphrey, C., Noonan, S., De'ath, G., Okazaki, R., Muehllehner, N., Glas, M. S., and Lough, J. M.: Losers and winners in coral reefs acclimatized to elevated carbon dioxide concentrations, *Nat. Clim. Change*, 1, 165–169, doi:10.1038/nclimate1122, 2011.
- Ferrier-Pages, C., Gattuso, J. P., Dallot, S., and Jaubert, J.: Effect of nutrient enrichment on growth and photosynthesis of the zooxanthellate coral *Stylophora pistillata*, *Coral Reefs*, 19, 103–113, doi:10.1007/S003380000078, 2000.
- Frieler, K., Meinshausen, M., Golly, A., Mengel, M., Lebek, K., Donner, S. D., and Hoegh-Guldberg, O.: Limiting global warming to 2C is unlikely to save most coral reefs, *Nature Climate Change*, 3, 165–170, doi:10.1038/nclimate1674, 2013
- Gattuso, J. P., Frankignoulle, M., Bourge, I., Romaine, S., and Buddemeier, R. W.: Effect of calcium carbonate saturation of seawater on coral calcification, *Global Planet. Change*, 18, 37–46, doi:10.1016/S0921-8181(98)00035-6, 1998.
- Gilchrist, G. W.: Specialists and generalists in changing environments, 1. Fitness landscapes of thermal sensitivity, *Am. Nat.*, 146, 252–270, doi:10.1086/285797, 1995.
- Grigg, R. W.: Coral reef development at high latitudes in Hawaii, in: *Proc. 4th Int. Coral Reef Symposium, Manila, Vol. 1*, 687–693, 1981.
- Gustafsson, M. S. M., Baird, M. E., and Ralph, P. J.: The interchangeability of autotrophic and heterotrophic nitrogen sources in Scleractinian coral symbiotic relationships: a numerical study, *Ecol. Model.*, 250, 183–194, doi:10.1016/j.ecolmodel.2012.11.003, 2013.

## Modeling coral calcification

C. Evenhuis et al.

Title Page

Abstract

Introduction

Conclusions

References

Tables

Figures

◀

▶

◀

▶

Back

Close

Full Screen / Esc

Printer-friendly Version

Interactive Discussion



- Halford, A. R. and Caley, M. J.: Towards an understanding of resilience in isolated coral reefs, *Glob. Change Biol.*, 15, 3031–3045, doi:10.1111/j.1365-2486.2009.01972.x, 2009.
- Hoegh-Guldberg, O., Mumby, P. J., Hooten, A. J., Steneck, R. S., Greenfield, P., Gomez, E., Harvell, C. D., Sale, P. F., Edwards, A. J., Caldeira, K., Knowlton, N., Eakin, C. M., Iglesias-Prieto, R., Muthiga, N., Bradbury, R. H., Dubi, A., and Hatziolos, M. E.: Coral reefs under rapid climate change and ocean acidification, *Science*, 318, 1737–1742, doi:10.1126/Science.1152509, 2007.
- Hoeye, R. K., Jokiel, P. L., Buddemeier, R. W., and Brainard, R. E.: Projected changes to growth and mortality of Hawaiian corals over the next 100 years, *Plos One*, 6, e18038, doi:10.1371/journal.pone.0018038, 2011.
- Holcomb, M., Cohen, A. L., and McCorkle, D. C.: An investigation of the calcification response of the scleractinian coral *Astrangia poculata* to elevated  $p\text{CO}_2$  and the effects of nutrients, zooxanthellae and gender, *Biogeosciences*, 9, 29–39, doi:10.5194/bg-9-29-2012, 2012.
- Houlbreque, F. and Ferrier-Pages, C.: Heterotrophy in tropical scleractinian corals, *Biol. Rev.*, 84, 1–17, doi:10.1111/j.1469-185X.2008.00058.x, 2009.
- Howells, E., Berkelmans, R., Van Oppen, M., Willis, B. L., and Bay, L.: Historical thermal regimes define limits to coral acclimatisation, *Ecology*, 94, 1078–1088, doi:10.1890/12-1257.1, 2013.
- Jokiel, P. L. and Coles, S. L.: Effects of temperature on mortality and growth of Hawaiian reef corals, *Mar. Biol.*, 43, 201–208, doi:10.1007/Bf00402312, 1977.
- Jokiel, P. L. and Guinther, E. B.: Effects of temperature on reproduction in the hermatypic coral *Pocillopora-Damicornis*, *B. Mar. Sci.*, 28, 786–789, 1978.
- Jones, R. J.: Coral bleaching, bleaching-induced mortality, and the adaptive significance of the bleaching response, *Mar. Biol.*, 154, 65–80, doi:10.1007/S00227-007-0900-0, 2008.
- Jones, R. J., Hoegh-Guldberg, O., Larkum, A. W. D., and Schreiber, U.: Temperature-induced bleaching of corals begins with impairment of the  $\text{CO}_2$  fixation mechanism in zooxanthellae, *Plant Cell Environ.*, 21, 1219–1230, doi:10.1046/J.1365-3040.1998.00345.X, 1998.
- Key, R. M., Kozyr, A., Sabine, C. L., Lee, K., Wanninkhof, R., Bullister, J., Feely, R. A., Millero, F., Mordy, C., and Peng, T.-H.: A global ocean carbon climatology: results from Global Data Analysis Project (GLODAP), *Global Biogeochem. Cy.*, 18, GB4031, doi:10.1029/2004GB002247, 2004.

## Modeling coral calcification

C. Evenhuis et al.

Title Page

Abstract

Introduction

Conclusions

References

Tables

Figures

◀

▶

◀

▶

Back

Close

Full Screen / Esc

Printer-friendly Version

Interactive Discussion



Kinzie, R. A., Takayama, M., Santos, S. R., and Coffroth, M. A.: The adaptive bleaching hypothesis: experimental tests of critical assumptions, *Biol. Bull.*, 200, 51–58, doi:10.2307/1543084, 2001.

Kleypas, J. A., Feely, R. A., Fabry, V. J., Langdon, C., Sabine, C. L., and Robbins, L. L.: Impacts of Ocean Acidification on Coral Reefs and Other Marine Calcifiers, A Guide for Future Research, Report of a workshop sponsored by NSF, NOAA & USGS, 2006.

Kleypas, J. A. and Langdon, C.: Coral reefs and changing seawater carbonate chemistry, *Coast. Estuar. Stud.*, 61, 73–110, 2006.

Langdon, C. and Atkinson, M. J.: Effect of elevated  $p\text{CO}_2$  on photosynthesis and calcification of corals and interactions with seasonal change in temperature/irradiance and nutrient enrichment, *J. Geophys. Res.*, 110, C09S07, doi:10.1029/2004jc002576, 2005.

Le Quéré, C., Andres, R. J., Boden, T., Conway, T., Houghton, R. A., House, J. I., Marland, G., Peters, G. P., van der Werf, G. R., Ahlström, A., Andrew, R. M., Bopp, L., Canadell, J. G., Ciais, P., Doney, S. C., Enright, C., Friedlingstein, P., Huntingford, C., Jain, A. K., Jourdain, C., Kato, E., Keeling, R. F., Klein Goldewijk, K., Levis, S., Levy, P., Lomas, M., Poulter, B., Raupach, M. R., Schwinger, J., Sitch, S., Stocker, B. D., Viovy, N., Zaehle, S., and Zeng, N.: The global carbon budget 1959–2011, *Earth Syst. Sci. Data*, 5, 165–185, doi:10.5194/essd-5-165-2013, 2013.

Leclercq, N., Gattuso, J. P., and Jaubert, J.:  $\text{CO}_2$  partial pressure controls the calcification rate of a coral community, *Glob. Change Biol.*, 6, 329–334, doi:10.1046/J.1365-2486.2000.00315.X, 2000.

Leclercq, N., Gattuso, J. P., and Jaubert, J.: Primary production, respiration, and calcification of a coral reef mesocosm under increased  $\text{CO}_2$  partial pressure, *Limnol. Oceanogr.*, 47, 558–564, 2002.

Lima, F. P. and Wetthey, D. S.: Three decades of high-resolution coastal sea surface temperatures reveal more than warming, *Nat. Commun.*, 3, 704, doi:10.1038/Ncomms1713, 2012.

Lough, J. and Barnes, D.: Several centuries of variation in skeletal extension, density and calcification in massive *Porites* colonies from the Great Barrier Reef: a proxy for seawater temperature and a background of variability against which to identify unnatural change, *J. Exp. Mar. Biol. Ecol.*, 211, 29–67, 1997.

Lough, J. and Barnes, D.: Environmental controls on growth of the massive coral *Porites*, *J. Exp. Mar. Biol. Ecol.*, 245, 225–243, 2000.

## Modeling coral calcification

C. Evenhuis et al.

Title Page

Abstract

Introduction

Conclusions

References

Tables

Figures

◀

▶

◀

▶

Back

Close

Full Screen / Esc

Printer-friendly Version

Interactive Discussion



- Lough, J. M.: Coral calcification from skeletal records revisited, *Mar. Ecol.-Prog. Ser.*, 373, 257–264, doi:10.3354/Meps07398, 2008.
- Lough, J. M.: Small change, big difference: sea surface temperature distributions for tropical coral reef ecosystems, 1950–2011, *J. Geophys. Res.*, 117, C09018, doi:10.1029/2012JC008199, 2012.
- 5 Marshall, P. and Baird, A.: Bleaching of corals on the Great Barrier Reef: differential susceptibilities among taxa, *Coral reefs*, 19, 155–163, 2000.
- Marubini, F., Barnett, H., Langdon, C., and Atkinson, M. J.: Dependence of calcification on light and carbonate ion concentration for the hermatypic coral *Porites compressa*, *Mar. Ecol.-Prog. Ser.*, 220, 153–162, doi:10.3354/Meps220153, 2001.
- 10 Marubini, F., Ferrier-Pagès, C., Furla, P., and Allemand, D.: Coral calcification responds to sea-water acidification: a working hypothesis towards a physiological mechanism, *Coral Reefs*, 27, 491–499, doi:10.1007/s00338-008-0375-6, 2008.
- Muller, E. B., Kooijman, S. A., Edmunds, P. J., Doyle, F. J., and Nisbet, R. M.: Dynamic energy budgets in syntrophic symbiotic relationships between heterotrophic hosts and photoautotrophic symbionts, *J. Theor. Biol.*, 259, 44–57, 2009.
- 15 Nisbet, R. M., Muller, E. B., Lika, K., and Kooijman, S. A. L. M.: From molecules to ecosystems through dynamic energy budget models, *J. Anim. Ecol.*, 69, 913–926, doi:10.1046/J.1365-2656.2000.00448.X, 2000.
- 20 Ohde, S. and Hossain, M. M. M.: Effect of CaCO<sub>3</sub> (aragonite) saturation state of seawater on calcification of *Porites* coral, *Geochem. J.*, 38, 613–621, 2004.
- Oliver, T. and Palumbi, S.: Do fluctuating temperature environments elevate coral thermal tolerance?, *Coral Reefs*, 30, 429–440, 2011.
- Pandolfi, J. M., Connolly, S. R., Marshall, D. J., and Cohen, A. L.: Projecting coral reef futures under global warming and ocean acidification, *Science*, 333, 418–422, doi:10.1126/science.1204794, 2011.
- 25 Poulsen, A., Burns, K., Lough, J., Brinkman, D., and Delean, S.: Trace analysis of hydrocarbons in coral cores from Saudi Arabia, *Org. Geochem.*, 37, 1913–1930, doi:10.1016/J.Orggeochem.2006.07.011, 2006.
- 30 Putron, S. J., McCorkle, D. C., Cohen, A. L., and Dillon, A. B.: The impact of seawater saturation state and bicarbonate ion concentration on calcification by new recruits of two Atlantic corals, *Coral Reefs*, 30, 321–328, doi:10.1007/s00338-010-0697-z, 2010.

## Modeling coral calcification

C. Evenhuis et al.

Title Page

Abstract

Introduction

Conclusions

References

Tables

Figures

◀

▶

◀

▶

Back

Close

Full Screen / Esc

Printer-friendly Version

Interactive Discussion



Rayner, N., Parker, D., Horton, E., Folland, C., Alexander, L., Rowell, D., Kent, E., and Kaplan, A.: Global analyses of sea surface temperature, sea ice, and night marine air temperature since the late nineteenth century, *J. Geophys. Res.-Atmos.*, 108, 4407, doi:10.1029/2002JD002670, 2003.

5 Reynolds, R. W., Smith, T. M., Liu, C., Chelton, D. B., Casey, K. S., and Schlax, M. G.: Daily high-resolution-blended analyses for sea surface temperature, *J. Climate*, 20, 5473–5496, doi:10.1175/2007jcli1824.1, 2007.

Ricke, K. L., Orr, J. C., Schneider, K., and Caldeira, K.: Risks to coral reefs from ocean carbonate chemistry changes in recent earth system model projections, *Environ. Res. Lett.*, 8, 034003, doi:10.1088/1748-9326/1088/1083/034003, 2013.

10 Ries, J. B., Cohen, A. L., and McCorkle, D. C.: A nonlinear calcification response to CO<sub>2</sub>-induced ocean acidification by the coral *Oculina arbuscula*, *Coral Reefs*, 29, 661–674, doi:10.1007/s00338-010-0632-3, 2010.

Rodrigues, L. J. and Grottoli, A. G.: Calcification rate and the stable carbon, oxygen, and nitrogen isotopes in the skeleton, host tissue, and zooxanthellae of bleached and recovering Hawaiian corals, *Geochim. Cosmochim. Ac.*, 70, doi:10.1016/j.gca.2006.02.014, 2006.

Schneider, K. and Erez, J.: The effect of carbonate chemistry on calcification and photosynthesis in the hermatypic coral *Acropora eurystroma*, *Limnol. Oceanogr.*, 51, 1284–1293, 2006.

20 Scoffin, T., Tudhope, A., Brown, B., Chansang, H., and Cheeney, R.: Patterns and possible environmental controls of skeletogenesis of *Porites lutea*, South Thailand, *Coral Reefs*, 11, 1–11, 1992.

Shaw, E. C., McNeil, B. I., and Tilbrook, B.: Impacts of ocean acidification in naturally variable coral reef flat ecosystems, *J. Geophys. Res.*, 117, C3038, doi:10.1029/2011jc007655, 2012.

25 Shi, Q., Yu, K. F., Chen, T. R., Zhang, H. L., Zhao, M. X., and Yan, H. Q.: Two centuries-long records of skeletal calcification in massive *Porites* colonies from Meiji Reef in the southern South China Sea and its responses to atmospheric CO<sub>2</sub> and seawater temperature, *Sci. China Earth Sci.*, 55, 1–12, doi:10.1007/S11430-011-4320-0, 2012.

Silverman, J., Lazar, B., Cao, L., Caldeira, K., and Erez, J.: Coral reefs may start dissolving when atmospheric CO<sub>2</sub> doubles, *Geophys. Res. Lett.*, 36, L05606, doi:10.1029/2008gl036282, 2009.

30 Stearns, S. C.: The evolutionary significance of phenotypic plasticity, *Bioscience*, 39, 436–445, 1998.

Tambutte, E., Tambutte, S., Segonds, N., Zoccola, D., Venn, A., Erez, J., and Allemand, D.: Calcein labelling and electrophysiology: insights on coral tissue permeability and calcification, Proc. R. Soc. B, 279, 19–27, 2012.

5 van Hooidonk, R., Maynard, J. A., and Planes, S.: Temporary refugia for coral reefs in a warming world, Nature Climate Change, 3, 503–511, doi:10.1038/nclimate1829, 2013.

Wilkinson, C.: Status of the coral reefs of the world, Global Coral Reef Monitoring Network and Reef And Rainforest Research Centre, Townsville, Australia, 296, 2008.

## BGD

11, 187–249, 2014

### Modeling coral calcification

C. Evenhuis et al.

Title Page

Abstract

Introduction

Conclusions

References

Tables

Figures

⏪

⏩

◀

▶

Back

Close

Full Screen / Esc

Printer-friendly Version

Interactive Discussion



## Modeling coral calcification

C. Evenhuis et al.

Title Page

Abstract

Introduction

Conclusions

References

Tables

Figures

◀

▶

◀

▶

Back

Close

Full Screen / Esc

Printer-friendly Version

Interactive Discussion



**Table 1.** Source data for experimental results in Fig. 1.

Plateau		Linear	
a	Holcomb et al. (2012)	1	Holcomb et al. (2012)
b	Langdon and Atkinson (2005)	2	Langdon and Atkinson (2005)
c	Leclercq et al. (2000)	3	Schneider and Erez (2006)
d	Leclercq et al. (2002)	4	Broecker et al. (2001)
e	Ries et al. (2010)	5	Andersson et al. (2009)
f	Marubini et al. (2001)	6	Albright et al. (2008)
g	Marubini et al. (2008)	7	Erez et al. (2011)
h	Gattuso et al. (1998)	8	Shaw et al. (2012)
i	de Putron et al. (2011)	9	Ohde and Hossain (2004)

## Modeling coral calcification

C. Evenhuis et al.

Title Page

Abstract

Introduction

Conclusions

References

Tables

Figures

◀

▶

◀

▶

Back

Close

Full Screen / Esc

Printer-friendly Version

Interactive Discussion



**Table 2.** Estimated growth constants for the corals after bleaching events from published studies.

Growth Rate $d^{-1}$	Type of experiment	Timescale	Reference
0.0200	Reproduction in laboratory	months	Jokiel and Coles (1977)
0.0020–0.0080	Weight increase in nubbins	months	Ferrier-Pages et al. (2000)
0.0100	Regen. of a bleached reef overlap with recovery)	Years	Diaz-Pulido et al. (2009)
0.0025–0.0010	Regen. of a bleached reef	Years	Brown and Suharsono (1990)
0.0020	Regen. of a bleached reef	Years	Baker et al. (2008)
0.0020	Regen. of a bleached reef	Years	Baker et al. (2008)
0.0015–0.0007	10–20 yr recovery estimate	Years	Coles and Brown (2007)
0.0010	Regen. of a bleached reef	Years	Adjeroud et al. (2009)
0.0010	Regen. of a bleached reef	Years	Ceccarelli et al. (2011)
0.0008	Regen. of a bleached reef	Years	Halford and Caley (2009)

**BGD**

11, 187–249, 2014

**Modeling coral calcification**

C. Evenhuis et al.

[Title Page](#)[Abstract](#)[Introduction](#)[Conclusions](#)[References](#)[Tables](#)[Figures](#)[I◀](#)[▶I](#)[◀](#)[▶](#)[Back](#)[Close](#)[Full Screen / Esc](#)[Printer-friendly Version](#)[Interactive Discussion](#)**Table 3.** The correspondence between the reported bleaching states by Baird and Marshall (2002) and the modelling states.

Model	Observation
Normal + Recovering	Normal + 1–10 %
Pale	11–50 % + 55–99 %
Bleached	100 %
Dead	Dead

## Modeling coral calcification

C. Evenhuis et al.

**Table 4.** Estimates for the adapted temperature range for the central and southern GBR sites in the reciprocal transplant experiment of Howells (2013). The thresholds are calculated using a variety of methods and from two SST records. The empirically derived thresholds (bolded) are used in model run shown in Fig. 11.

	Method		Central		Southern	
			NOAA	In situ	NOAA	In situ
Upper Threshold	Percentile	99.9th	30.9	31.6	29.3	29.9
	Climatology	Feb $\mu + 2.45\sigma$	31.2	32.7	30.2	29.5
	Optimised	$T_{hi}$	31.6		30.3	
	Empirical	$T_{hi}$		<b>31.8</b>		<b>30.3</b>
Lower Threshold	Percentile	0.1th	20.3	19.4	18.6	18.5
	Climatology	Jul $\mu - 2.45\sigma$	20.2	19.3	18.5	18.0
	Optimised	$T_{lo}$	19.7		18.0	
	Empirical	$T_{lo}$		<b>20.0</b>		<b>18.2</b>

Title Page

Abstract

Introduction

Conclusions

References

Tables

Figures

I ◀

▶ I

◀

▶

Back

Close

Full Screen / Esc

Printer-friendly Version

Interactive Discussion



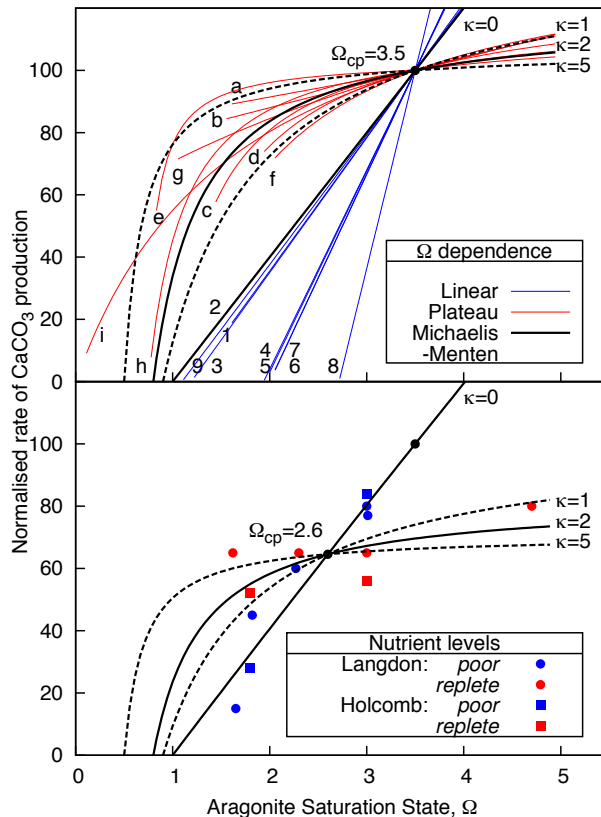


**Fig. 1.** Comparison of the responses of coral to Aragonite saturation state with the modified Michaelis–Menten curve from Eq. (2) plotted for linear response ( $\kappa = 0$ , solid) and for plateaued responses ( $\kappa = 1, 2, 5$ , dashed, solid, dashed). Upper panel: curves are fitted to experimental data and normalised to present day values of  $\Omega = 3.5$ , is plotted with  $\Omega_{cp} = 3.5$ . Lower panel: results from the nutrient manipulation experiments of Holcomb et al. (2012) and Langdon (2005) are plotted with Eq. (2) for  $\Omega_{cp} = 2.6$ .

Title Page

Abstract Introduction

Conclusions References

Tables Figures

◀ ▶

◀ ▶

Back Close

Full Screen / Esc

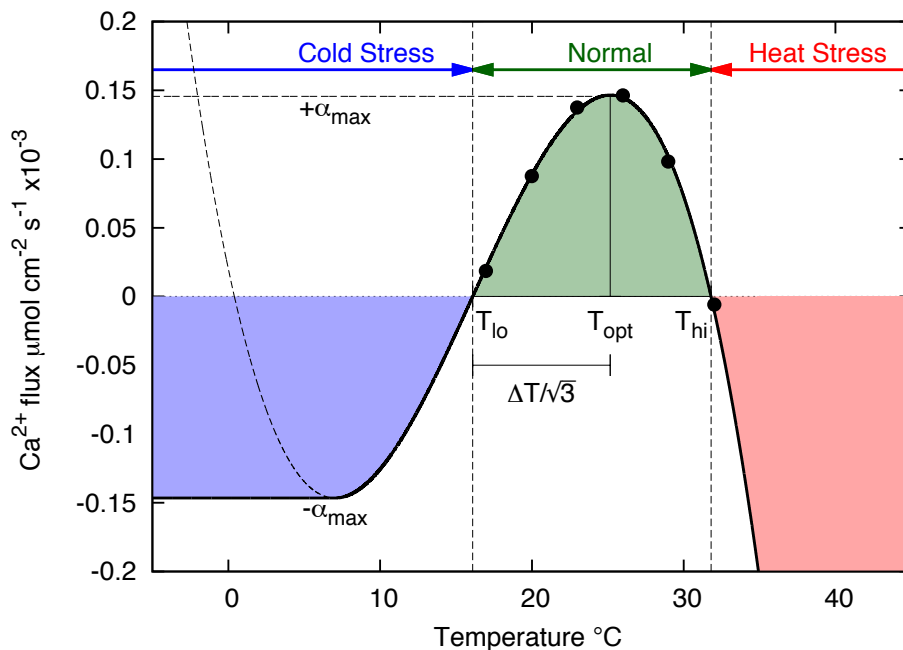
Printer-friendly Version

Interactive Discussion



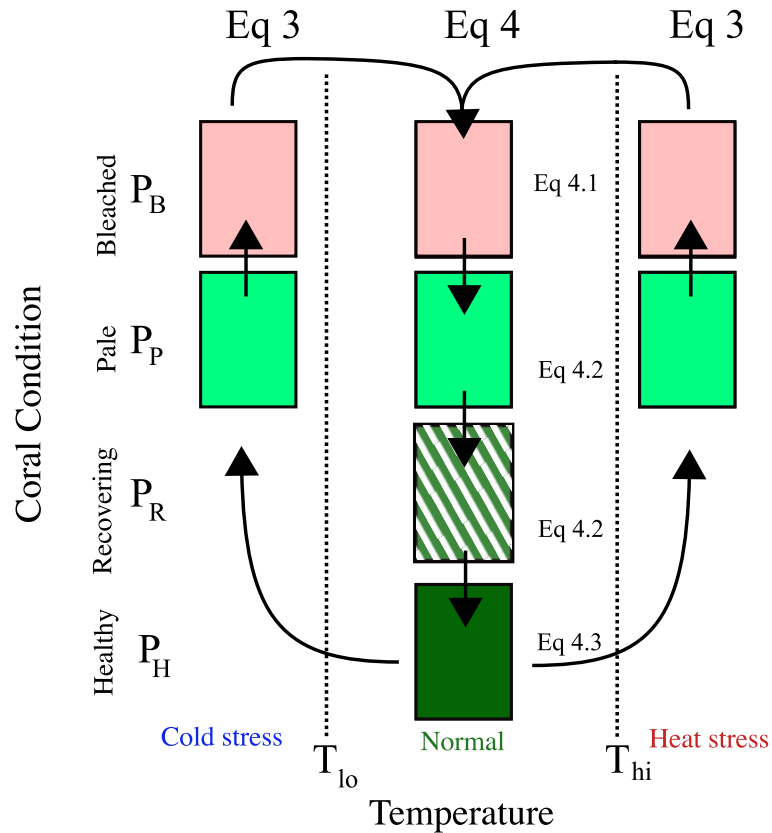
## Modeling coral calcification

C. Evenhuis et al.

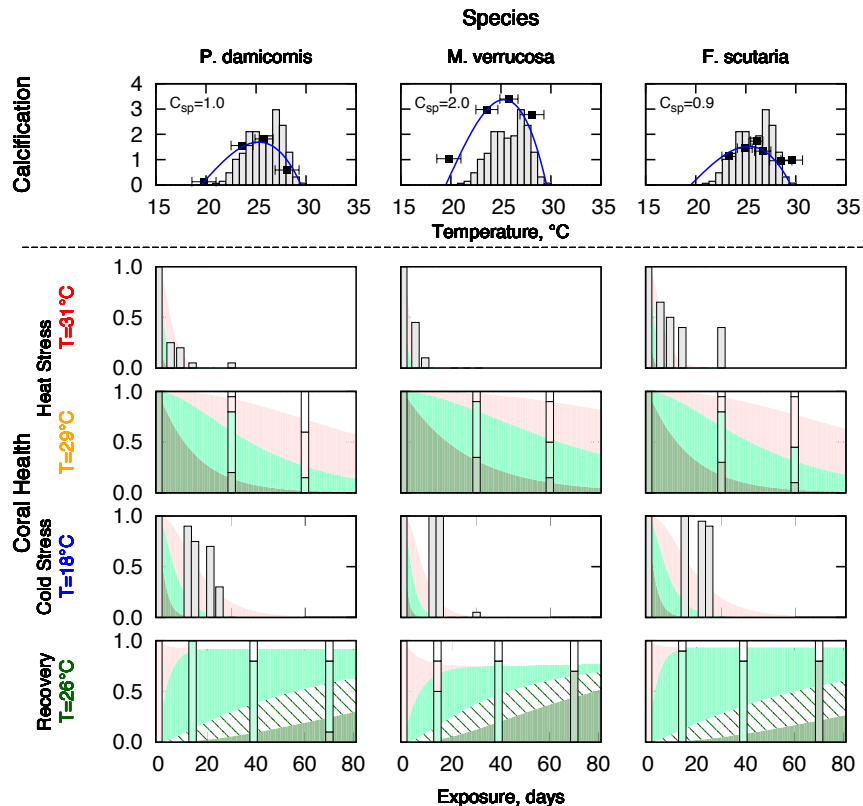


**Fig. 2.** The functional form of adapted response (thick black line) fitted to experimental data of Al-Horani (2005) (black circles). The adapted temperature range is shown in green and the temperatures at which heat stress and cold stress occur are shown in red and blue.

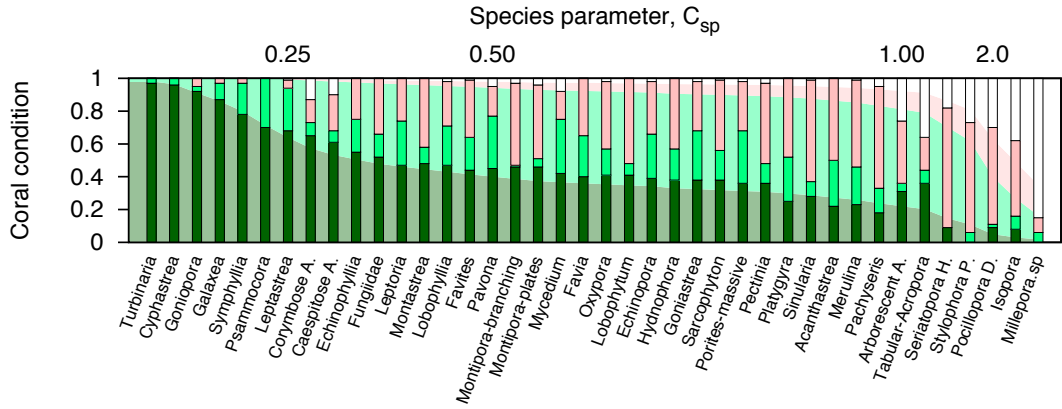
[Title Page](#)
[Abstract](#)
[Introduction](#)
[Conclusions](#)
[References](#)
[Tables](#)
[Figures](#)
[◀](#)
[▶](#)
[◀](#)
[▶](#)
[Back](#)
[Close](#)
[Full Screen / Esc](#)
[Printer-friendly Version](#)
[Interactive Discussion](#)

**Fig. 3.** The 4 states of coral health in the model (Healthy, Recovering, Pale and Bleached), the transitions between the 4 states are represented by the directional arrows, and the arrow size gives an indication of the relative rates of the processes.



**Fig. 4.** Comparison of the simulated results with those observed by Jokiel and Coles (1977). The first row is the observed calcification rates (box and whiskers), the histogram of temperatures (grey boxes) and the adapted response curve (blue line). The lower 4 rows show the observations of the coral health as bars. When coral health was reported, the bars are coloured as in Fig. 3, otherwise when only the total population was reported the bars are coloured grey. The model results are shown as continuous fill using the colour scheme of Fig. 3.



**Fig. 5.** Comparison of the observed bleaching in coral on the Great Barrier Reef from Marshall and Baird (2000) with modelled bleaching as a function of the species parameter,  $C_{sp}$ .

Title Page

Abstract Introduction

Conclusions References

Tables Figures

◀ ▶

◀ ▶

Back Close

Full Screen / Esc

Printer-friendly Version

Interactive Discussion



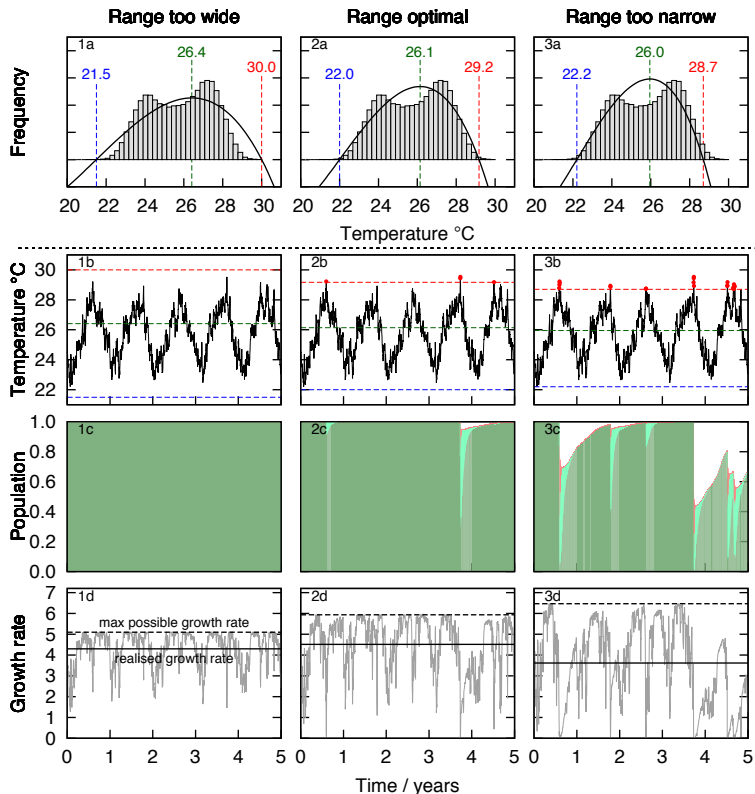


**Fig. 6.** An illustration of how the temperature ranges ( $T_{lo}$ ,  $T_{hi}$ ) are found by optimising the calcification over an historical temperature record. The first row shows the histogram of the historical temperature with the transient temperature curve and the key temperatures ( $T_{lo}$ ,  $T_{hi}$ ,  $T_{opt}$ ). The second row shows times series of the SSTs together with the key temperatures. Bleaching events are marked with red dots. The third row shows the condition of the coral (colouring as Fig. 3) and the calcification rate as a function of time.

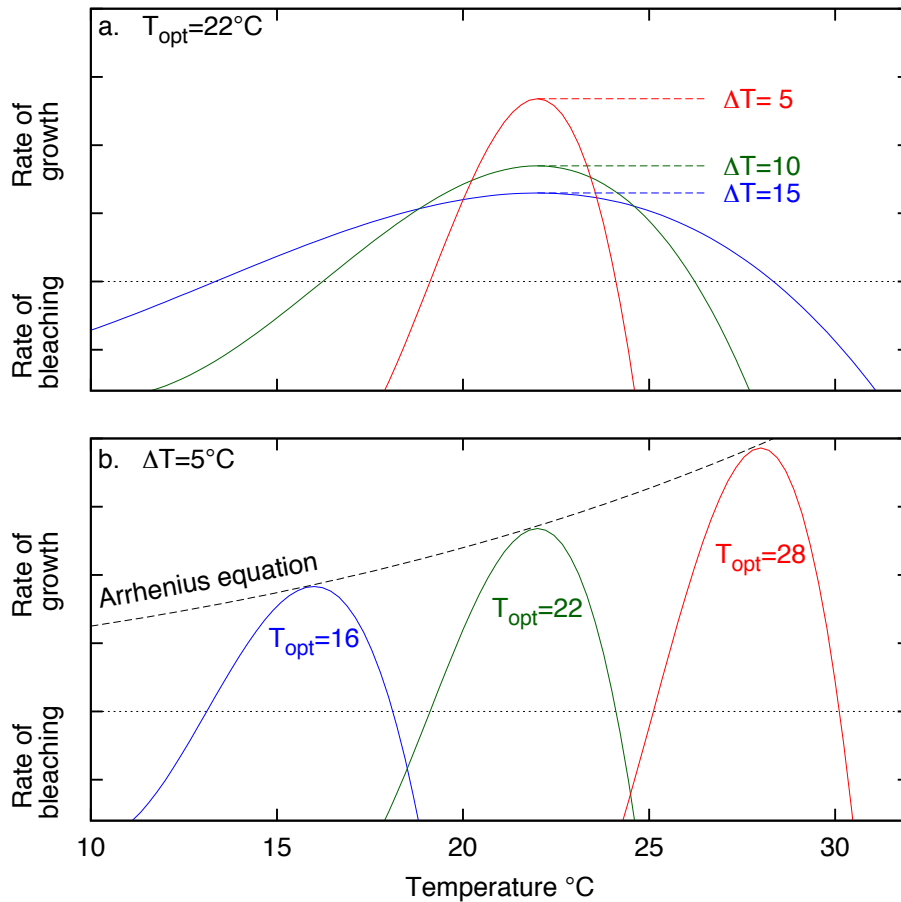


**Fig. 7.** An illustration of the temperature dependence of biological processes in the model. **(a)** (upper) shows the effect of changing the temperature range  $\Delta T$  while holding  $T_{opt}$  fixed. **(b)** (lower) shows the effect of changing  $T_{opt}$  whilst holding  $\Delta T$  fixed.

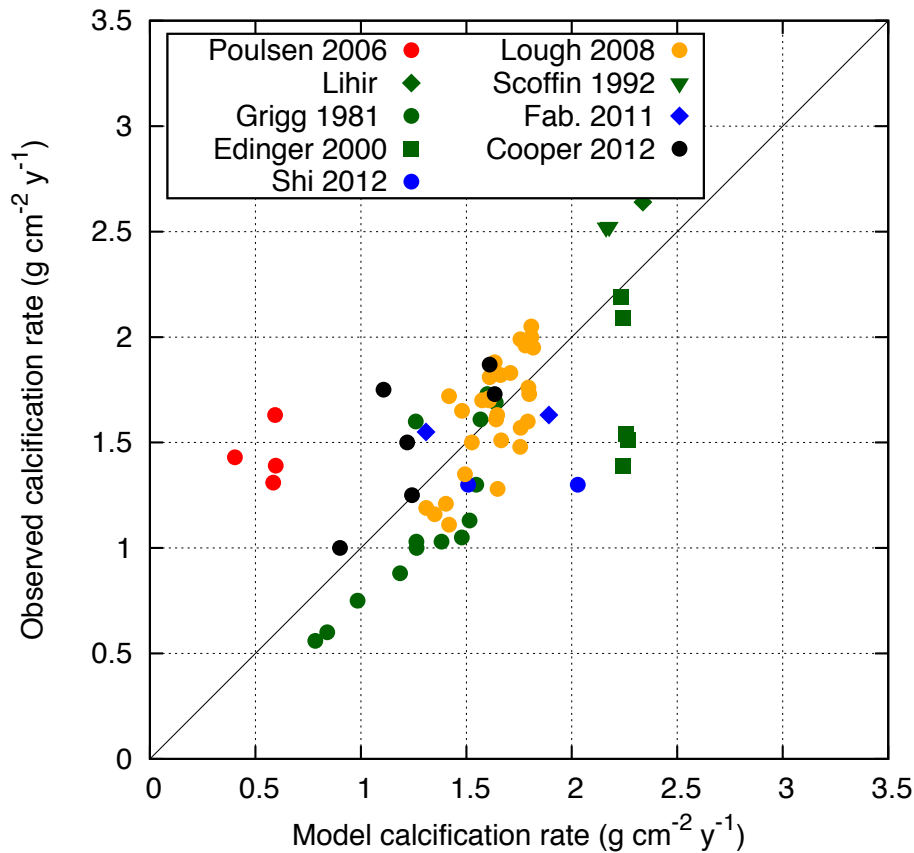


**Fig. 8.** Comparison between the observed and simulated calcification rates of *Porites* from 60 unique geographic locations. The Lahir datum is the calcification rate reported for Lahir Island, Papua New Guinea by Lough (2008).

Title Page

Abstract Introduction

Conclusions References

Tables Figures

◀ ▶

◀ ▶

Back Close

Full Screen / Esc

Printer-friendly Version

Interactive Discussion



## Modeling coral calcification

C. Evenhuis et al.

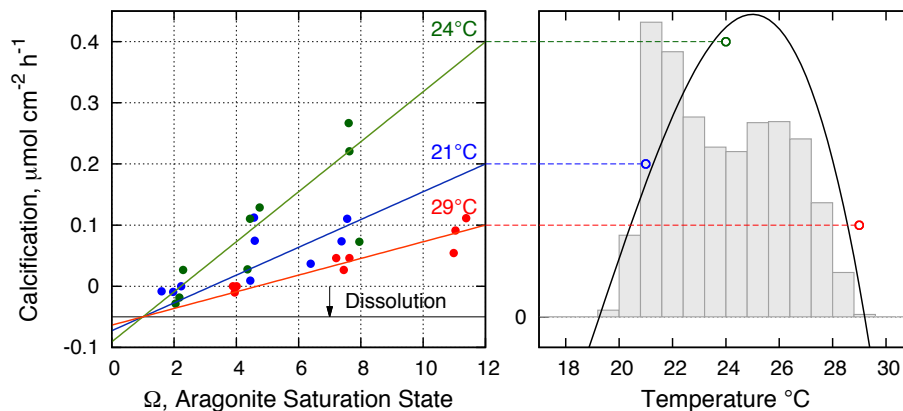


**Fig. 9.** Left panel, calcification rate for *Acropora eurystroma* as a function of Aragonite saturation state and temperature from Erez et al. (2011). The right panel shows the histogram of daily SSTs for the Gulf of Aqaba from the NOAA pathfinder product (grey bars). The dashed lines connecting the left and right panels of Fig. 9 shows the dependence of calcification rate on both the aragonite saturation state and temperature.

[Title Page](#)
[Abstract](#)
[Introduction](#)
[Conclusions](#)
[References](#)
[Tables](#)
[Figures](#)
[◀](#)
[▶](#)
[◀](#)
[▶](#)
[Back](#)
[Close](#)
[Full Screen / Esc](#)
[Printer-friendly Version](#)
[Interactive Discussion](#)


## Modeling coral calcification

C. Evenhuis et al.

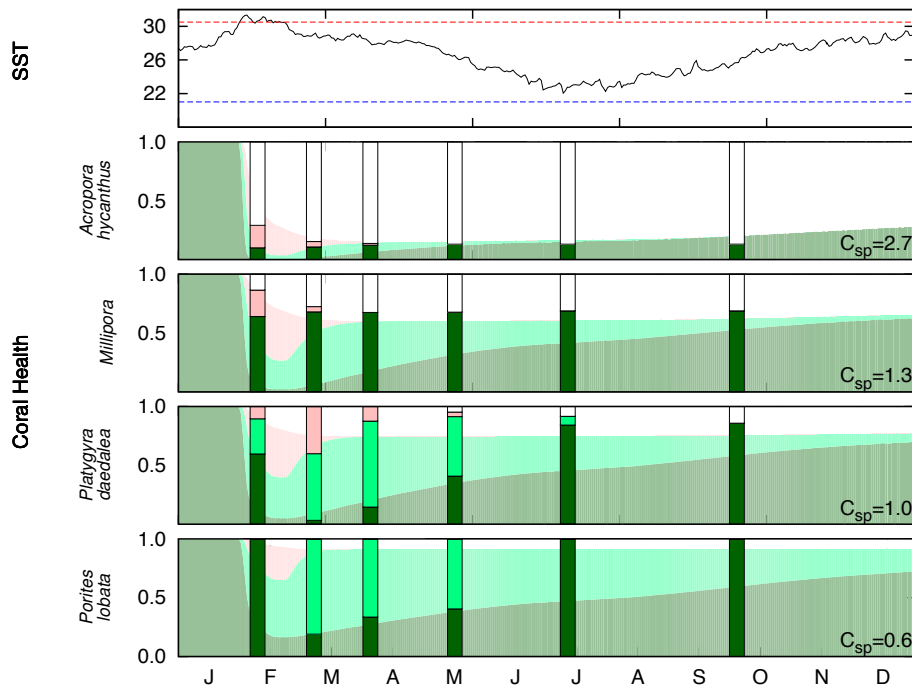


**Fig. 10.** The upper panel shows the mean daily SST from insitu observations and the adapted range (red and blue dashed lines). The lower panels show the comparison between the observed (bars; (Baird and Marshall, 2002)) and simulated coral bleaching and recovery for four different species.

Title Page

Abstract

Introduction

Conclusions

References

Tables

Figures

◀

▶

◀

▶

Back

Close

Full Screen / Esc

Printer-friendly Version

Interactive Discussion



## Modeling coral calcification

C. Evenhuis et al.

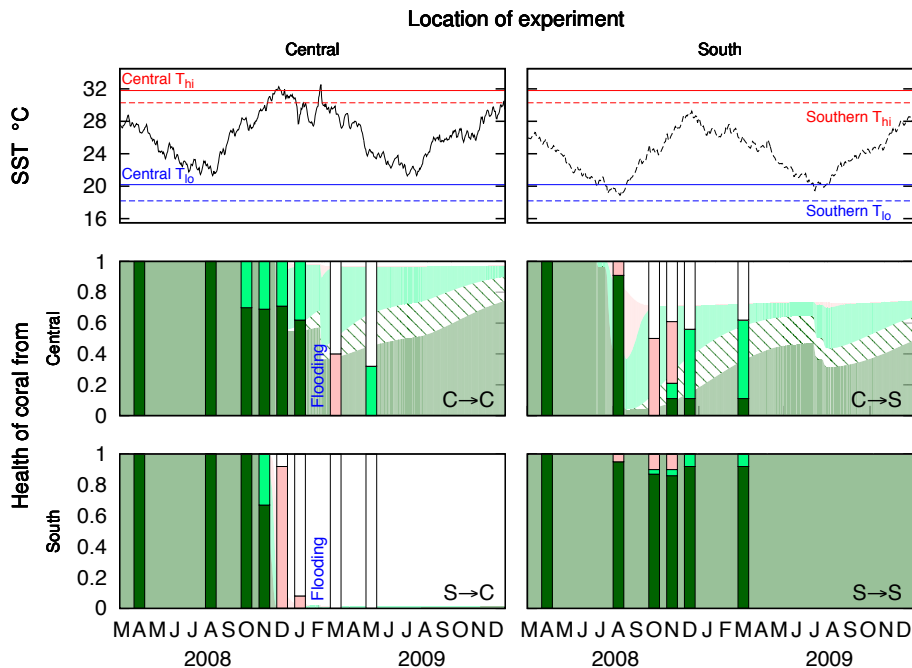


**Fig. 11.** Comparison of model runs with reciprocal coral transplant experiment (Howells et al., 2013). Top panels show SST in the central GBR (top left) and southern GBR (top right). The adapted ranges are shown for both locations, the dashed line representing the adapted range for the Southern GBR and the solid lines the adapted range of the Central GBR. The lower 4 panels show observed coral health (bars) and the model coral health (continuous fill) for the 4 experiments using the colour scheme of Fig. 3. The 4 experiments are: central corals remaining at the central GBR (centre left), central corals transplanted to southern GBR (centre right), southern corals transplanted to the central GBR (bottom left) and southern corals remaining on the southern GBR (bottom right).

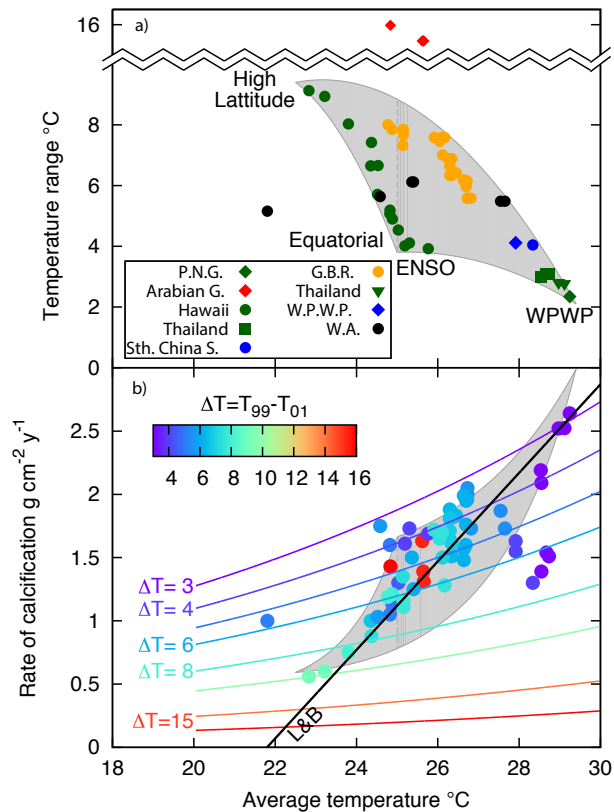


**Fig. 12.** The upper figure shows the average and range of SST from the 0.25° NOAA SST (Reynolds et al., 2007) for each location of the coral. The family of Arrhenius curves in the lower figure maps out a large area of possible calcification rates, while the symbols colors show the adapted range. Overlain on this plot is the linear relationship of Lough (2008). WPWP – refers to the Western Pacific Warm Pool; PNG – Papua New Guinea; W.A. Western Australia; and GBR Great Barrier Reef.